

9 This is a Preprint for a manuscript submitted to *Marine and Petroleum Geology* on the 15 November 2017

10 **Seismic and structural characterization of a pre-salt rifted section: the Lagoa**  
11 **Feia Group, Campos Basin, offshore Brazil**

12 **Iacopini D<sup>1\*</sup>, Alvarenga R. S.<sup>2</sup>, Kuchle J<sup>2</sup>, Cawood A. J.<sup>1</sup>, Goldberg K<sup>2</sup>, Kneller B<sup>1</sup>,**

13 1 School of Geosciences, University of Aberdeen, UK

14 2 Instituto de Geociências, BG Rift Lab, Universidade Federal do Rio Grande do Sul, Porto Alegre, Brazil

15

16

17 • Correspondence [d.iacopini@abdn.ac.uk](mailto:d.iacopini@abdn.ac.uk)

18

19

20

21

22 *This is a Preprint for a manuscript submitted to Marine and Petroleum Geology on 15 November 2017*

23

24 *12751 words, 13 figures, 52 references*

25 *Running head: Seismic and structural characterization of a pre-salt rifted section*

26 *Supplementary materials: None included*

27

28

29

30

31

32

33

34

# 35 Seismic and structural characterization of a pre-salt rifted section: the Lagoa 36 Feia Group, Campos Basin, offshore Brazil

37 Iacopini D<sup>1</sup>, Alvarenga R. S.<sup>2</sup>, Kuchle J<sup>2</sup>, Cawood A. J. <sup>1</sup>, Goldberg K<sup>2</sup>, Kneller B<sup>1</sup>,

38 <sup>1</sup> School of Geosciences, University of Aberdeen, UK

39 <sup>2</sup> Instituto de Geociências, BG Rift Lab, Universidade Federal do Rio Grande do Sul, Porto Alegre, Brazil

## 40 41 42 **Abstract**

43 The Exploration and development of what it is commonly known the “pre-salt” layer, offshore SE  
44 Brazil, is in its infancy but with reservoirs buried below as much as 3000 meter of salt, the pre-salt play  
45 presents a multifaceted deep-water scenario that is bringing new challenges to seismic interpretation in  
46 offshore Brazilian exploration and production. Reservoirs in this domain are complex, heterogeneous  
47 with layered carbonates which makes accurate reservoir characterization very challenging. Our study  
48 here deals with the seismic characterization of the stratigraphy of a lacustrine section from the Lagoa  
49 Feia Group (Winter et al., 2007) in the Campos Basin, which extends over an area of 100,000 km<sup>2</sup>. By  
50 using the existing 2D seismic dataset and two deep well logs and core information, we propose a seismic  
51 facies analysis and structural characterization of the Lagoa Feia formation. Using some simplified  
52 kinematic restoration we show that some of the normal faults affecting the lower units of the Lagoa  
53 Feia could be interpreted as pre rift structures *sensu lato* but also as pre-existing structures re-activated  
54 during the main passive margin rift activities. Inferences from well core and seismic stratigraphy clearly  
55 suggest that the all Lagoa Feia group has a syn rift depositional character. Different pre- syn- and post-  
56 rift seismic stratigraphic units, with corresponding bounding surfaces are then defined. Based on their  
57 seismic character, four seismic facies representing the main lithological package in the rift section are  
58 recognized: border fault deposits; fine grain-dominated re-sedimented deposits; coarse grain-dominated  
59 carbonate rich re-sedimented deposits; and an intrusive wipe-out zone affecting all the pre-salt unit. By  
60 proposing this seismic classification and interpretation across the pre salt Campos Basin units this work  
61 represents an introductory step to a facies classification and structural interpretation applicable at  
62 regional level in the internal SE Brazil offshore area.

## 63 **1 Introduction**

64 The Campos Basin in eastern Brazil comprises an area of 100.000 km<sup>2</sup>, with more than 2900 drilled  
65 wells (Guardado et al., 2000; ANP-BDEP, 2015). Before the recent discoveries of the voluminous pre-  
66 salt accumulations, the basin corresponded to more than 90% of Brazil petroleum reserves (Winter et  
67 al., 2007). The Lagoa Feia Group, deposited in the rift and sag pre-salt phases, includes lacustrine  
68 organic-rich shales, which constitute the source rocks of the basin, and carbonate rocks, which

69 correspond to the main reservoir rocks of the rift section. Despite of the huge number of wells, only a  
70 few cores were taken on the rift section of the Lagoa Feia Group. Excluding cored intervals with less  
71 than 3 meters, cores of the rift section represent no more than 600 meters across the entire Campos  
72 Basin, usually with 10 to 15 continuous meters, taken at the shallow part of the basin. The area has been  
73 explored and investigated (Abrahão & Warne, 1990) and recently re-interpreted in detail from a  
74 petrologic-sedimentology perspective (Armelenti et al., 2016) and a stratigraphic-seismic point of view  
75 (Alvarenga et al., 2016; Goldberg et al, 2017) as re-sedimented gravitational deposits within a rift  
76 lacustrine environment . This paper builds on the petrographic, stratigraphic and sedimentological data  
77 and interpretation proposed by Armelenti, 2016; Alvarenga et al., 2016; Goldberg et al, 2017 and  
78 focuses on the seismic expression of the Lagoa Feia different formations and its structural relationship  
79 respect to the syn rift activity. We will discuss the seismic stratigraphy nature of the Lagoa Feia respect  
80 to the major normal fault affecting the pre salt system and some rift kinematic scenario for the internal  
81 area will be proposed accordingly. By extracting the main seismic reflection parameters (which include  
82 geometry, continuity, amplitude, frequency) and analysing some wire-line log data from wells that can  
83 be tied to the sub-salt seismic data, we will finally propose some main seismic facies that have regional  
84 significance across the Campos Basin for the Lagoa Feia Group.

## 85 **2 Geological and tectonic settings**

86 The Campos Basin, offshore Brazil, is situated on the south-eastern continental shelf part\_of the  
87 Brazilian offshore between the Cabo Frio High to the south and the Vitoria High to the north (Fig. 1).  
88 Like most of the Brazilian offshore basins, the Campos Basin was formed during the breakup of  
89 Gondwana and the drifting apart of South America and Africa in late Jurassic to Early Cretaceous time  
90 (Mohriak et al., 2008, Karner, 2000). Following Kumar et al., (1977) and Zalan et al., (2011) the  
91 sedimentary wedge in the Campos Basin is at least 4-6 km thick and locally thins out over some  
92 basement highs as shown in the regional section from the Campos area obtained from our mapping.  
93 During this major tectonic event both the Atlantic margin of Brazil and the west African margin  
94 experienced an extended deformation history, first involving deep-seated crustal deformation associated  
95 with Barremian-Aptian rifting, and subsequent sea floor spreading and drifting of the Atlantic margins  
96 (Mohriak, 2008). Refraction experiments (Zalan et al., 2011; Moulin et al., 2011) suggest that further  
97 east the Campos Basin overlies thinned continental crust. Finally following the deep rift structuration  
98 during the Cenozoic, deformation of the cover sequences has been mainly driven by gravity tectonics  
99 (Demercian et al., 1993, Davison, 2008). Within this tectonic framework, the sedimentary record since  
100 the Mesozoic in the Campos Basin has been traditionally (Winter et al., 2007) described in terms of  
101 three supersequences (figure 2): (1) Rift Supersequence, (2) Post-Rift Supersequence and (3) Drift  
102 Supersequence. In this paper we will abandon this traditional classification based on the new seismic  
103 data presented, which clearly suggests some inconsistencies with the current post rift supersequences  
104 interpretation.

105 (1) The Rift Supersequence within the Campos Basin corresponds to basalts and minor conglomerates  
106 of the Cabiúnas Formation (Hauterivian) and the lower portion of the Lagoa Feia Group defined by the  
107 Atafona, Coqueiros and Itabapoana formations (Winter et al., 2007). The Barremian aged Atafona  
108 Formation consist of siltstones, sandstones and lacustrine shales with a distinctive talc-stevensite  
109 mineralogy, interbedded thin lacustrine limestones; the overlying Coqueiros Formation is of upper  
110 Barremian to lower Aptian age (locally resting on the Jiquiá) and has been described as coquinas (“Unit  
111 D – Coquinas Sequence” of Rangel & Carminatti, 2000), but is in fact composed of rudstones and  
112 grainstones that are not located in a specific stratigraphic interval (see Goldberg et al, 2017). The  
113 Itabapoana Formation (alluvial fans/fan deltas proximally and lacustrine/lagoon sediments distally) is  
114 also of Barremian to lower Aptian age, laterally equivalent to Atafona and Coqueiros formations  
115 (Winter et al., 2007). (2) The Post-Rift Supersequence (Fig 2) comprises the upper part of the Lagoa  
116 Feia Group, including the upper Itabapoana Formation, laterally equivalent Gargau (dominantly marls  
117 and calcilutites) and Macabu (stromatolitic and laminated microbialites?), and the overlying Retiro  
118 Formation, which is characterized by evaporites composed of anhydrite, carnallite and halite/sylvite of  
119 Aptian age deposited in marine/lagoonal environment in an arid climate (Winter et al., 2007, Tedeschi  
120 et al., 2017 ). However, all these lithostratigraphic units are not chronostratigraphically and regionally  
121 consistent, being in fact related to specific depositional environments that varied substantially along the  
122 rift and across the Campos Basin (Stanton & Masini, 2013). Moreover the interpretation of the upper  
123 part of the Lagoa Feia Group, including the upper Itabapoana Formation, laterally equivalent Gargau  
124 (dominantly marls and calcilutites) and Macabu (stromatolitic and laminated microbialites?) as part of  
125 the post rift supersequence has now been questioned (and will be further questioned in this paper).  
126 These units can certainly be interpreted as still part of the pre salt syn rift (Goldberg et al., 2017) but  
127 have been interpreted by others as a sag formation (Karner & Gamboa, 2007). The halite of the Retiro  
128 Formation represents the clear post rift formation unit (Tedeschi et al; 2017) and is remobilized into  
129 salt domes and diapirs with amplitudes of up to 3000 meters or more, which cut the overlying  
130 stratigraphy (Rangel et al. 1994). The upper portion of the Retiro Formation displays a retrogradational  
131 pattern, representing an eustatic sea-level rise (Winter 2007; Davison, 2007). (3) The Drift  
132 Supersequence comprises marine sediments of the Macaé and Campos Groups deposited in a regime of  
133 thermal subsidence associated with gravity-dominated tectonics (Winter et al., 2007), dominantly  
134 evaporite remobilization. The Macaé Group (Lower Albian to Cenomanian) consists dominantly of  
135 limestones and marls, while the Campos Group (Turonian to Recent) consists dominantly of siliciclastic  
136 sediments, deposited in progressively deeper marine environment (Winter et al., 2007).

137

### 138 **3 Description of the Datasets:**

139 The subsurface dataset (acquired through the 1980s to 1990s) consists of a series of 2D seismic surveys  
140 with a total of 282 seismic lines (but few of them has been here selected as representative), and 40 wells

141 of which only 13 have well logs and two have core (referred to here as wells A and B, Fig 1). Before  
142 describing the main seismic units and their tectonostratigraphic interpretation, it is worth discussing  
143 some of the properties of the seismic dataset.

1441) Most of the seismic data (2D) released for the project (Fig 1) was acquired primarily for the purpose of  
145 imaging the supra-salt, post-rift sedimentary units. They represent pre stack time migrated seismic  
146 section. As a consequence, most of the seismic processing has been focused on imaging units above the  
147 salt while only secondary attention has been paid to the sub-salt units. In Figure 3a, a sample 2D line  
148 extracted from the survey is represented in terms of the frequency. It represents a three frequency  
149 decomposition Red Green Blue (RGB) blended image (20, 48, 60 Hertz frequencies) using a constant  
150 mean frequency/ total bandwidth ratio. The blended image indicates that the highest frequencies over  
151 40 Hertz (whitish colours pointed by the arrows) are clearly associated with the supra-salt unit while  
152 the sub-salt units related to the Lagoa Feia Group are restricted to values below the 30 Hertz. Using the  
153 check-shot information available within the Lagoa Feia Group (Fig 3), which yield measured velocities  
154 varying between 2.1 and 2.7 km/sec, and using the mean frequency distribution described in Figure 3,  
155 we can estimate a minimum and maximum tuning thickness that varies between 10 and 50 m. Figure  
156 3b shows the calibration of some reflectors using the well log B which clearly confirms the resolution  
157 values of 16-30 m (at best), supporting the frequency analysis.

1582) The frequency analysis (Figure 3a) also suggests that the sub-salt seismic quality impaired the use of  
159 some seismic attributes to recognize and map the main boundaries between the basement (here named  
160 Cabiúñas Formation) and the main sequence. In some cases, due to the very low frequencies, the seismic  
161 resolution was well above the required tuning thickness necessary to unravel the main internal variations  
162 or lateral continuity of the seismic facies, reducing our ability to interpret the internal architecture of  
163 the syn-rift deposit. It is worth noting that several of the available wells were originally drilled with the  
164 intention of investigating targets located in the supra-salt sediments. This implies that most of the check-  
165 shots do not reach the Lagoa Feia Group and most of the wells do not contain any core information  
166 about the lowest pre-salt unit of interest. Only 3 wells stored useful core information across the full  
167 dataset and only two could match the entire pre-salt sequence. Therefore most of our seismic texture  
168 analysis will be devoted to seismic lines that are tied to those wells (Fig 1).

1693) Interval and average velocities for part of the well has been obtained mostly from both the well log  
170 sonic log and the check shots released for this research activity. The velocities varies considerably  
171 within the Lagoa Feia different formations but an average two main packages have been recognized.  
172 The Unit right below the salt unit across the main upper syn-rift unit ( defined later as *high tectonic to*  
173 *low tectonic activities system*) show interval velocities varying between 2.7 to 3 km/sec. A second  
174 package, with an average velocity of 2.4 to 2.5 km/sec has been instead defined below the main thick  
175 re deposited carbonate rich units as suggested by the two interval velocities indicated in figure 3b (white  
176 values in figure 3b). The two packages are roughly represented in figure 5b respectively by the two

177 bold thick lines in light orange and dark grey. Those two average of velocities has been used to calculate  
178 the mean depth across the well as in indicated by white numbers in figure 5b.

## 179 **4. Method**

### 180 **4.1 Seismic facies analysis**

181 In the last thirty years exploration geoscientists has been advancing seismic processing and  
182 visualization technology with the aim of recognizing large scale geological features by visual inspection  
183 of seismic reflection patterns. These efforts have led to the development of concepts such as *seismic*  
184 *facies*, defined as mappable three-dimensional seismic units composed of groups of reflections whose  
185 parameters (amplitude, reflection geometry, continuity and wavelet frequency) differ from the  
186 surrounding units (Prather et al., 1998; Posamantier et al., 2003). The concept of seismic facies has  
187 often been linked to geologic interpretation as a function of the depositional environment and  
188 lithofacies. Once these seismic properties are shown to be systematically associated with specific  
189 geological features then they can be defined as seismic facies. The interpretation of seismic facies often  
190 first requires the existence of a large-scale framework of seismic sequence analysis defined through the  
191 recognition of main sequence boundaries. Within this framework it is then possible to insert genetically-  
192 related subunits by using seismic expression calibrated through well log information. The study and use  
193 of seismic attributes (post- and pre-stack attributes) have played a fundamental part in this seismic facies  
194 analysis process by developing a plethora of temporal, spatial and instantaneous physical attributes  
195 (Taner & Sheriff, 1977; Taner et al., 1994; Chopra & Marfurt, 2007, Alves et al. (2014) Marfurt (2015),  
196 Marfurt and Alves (2015)), with the aim of enhancing signal properties and specific textures of seismic  
197 units. Seismic facies have then been constrained through robust statistical procedure and also through  
198 the consistent cross-analysis of well log data. When the geological information is incomplete or non-  
199 existent, seismic facies analyses are called non-supervised (Duda et al., 2000) and are performed  
200 through unsupervised learning or clustering algorithms (De Matos et al., 2007); When geological  
201 information is used to tie the seismic facies to wells then the term supervised seismic facies can be  
202 applied. Efforts to define seismic facies have been undertaken within a variety of geological contexts,  
203 such as carbonate (Sarg & Schuelke, 2003; Colpaert et al., 2007), deep-water (Prather et al., 1998;  
204 Posamantier & Kolla, 2003) and fluvial depositional environments. In this contribution we aim to  
205 investigate the qualitative seismic response of several seismic units from a rift lake system of the  
206 Campos Basin (offshore NE Brazil).

207 After recognition and mapping of the main units within the Lagoa Feia Group at seismic scale, the main  
208 seismic character of the various syn- and post-rift sub-units has been further analysed. In order to  
209 recognise patterns across the seismic dataset, different complex attributes (*sensu* Taner & Sheriff, 1977)  
210 and attribute combinations have been applied. Specifically the use of some attributes, such as the  
211 sweetness (specially to highlight the rift basement/first infill), the reflection strength, cosine of the

212 phase, and relative acoustic impedance, have been crucial to resolve some of the internal seismic  
213 expression representing the main units of the Lagoa Feia. Before describing the main seismic facies  
214 recognized in this study, we will first briefly describe the various attributes utilized and outline their  
215 utility in resolving signal properties during seismic facies analysis. A summary of their properties and  
216 image visualization across the Campos Basin seismic data analysed is proposed in Figure 4.

217 1) Root mean Square amplitude (Taner & Sheriff, 1977): we define the RMS as the root mean  
218 square amplitude of the signal (also known as “instantaneous amplitude or envelope”),  
219 calculated by taking the root of the summation of the squared real components of the signal.  
220 It is similar (but analytically not equivalent) to the RMS amplitude as it highlights, by doing  
221 the square rooted amplitude, the various anomalies within the seismic datasets. RMS is  
222 amplitude independent of phase attributes, it is always positive, and has the same range of  
223 squared values as the amplitude from which it is derived. To appreciate the main  
224 description and effect refer to the table in Figure 4.

225 2) Cosine of the phase (Taner & Sheriff, 1977): The instantaneous phase is defined as the  
226 tangent of the argument of any complex signal. The cosine of phase strictly derives from  
227 it, as it represents the cosine of the instantaneous phase. This attribute is of central  
228 importance, since it describes the location of events in the seismic trace and leads to the  
229 computation of other instantaneous quantities. It also makes strong events clearer and is  
230 effective at highlighting discontinuities of reflectors, faults, pinch-outs, angularities and  
231 bed interfaces. Seismic sequence boundaries, sedimentary layer patterns and regions of  
232 onlap/offlap patterns often exhibit extra clarity by using this attribute.

233 3) Sweetness (Radovich et al., 1998; Hart, 2008): the sweetness is derived mathematically by  
234 dividing reflection strength by the square root of instantaneous frequency. The  
235 instantaneous frequency is the rate of change of phase, has units of Hertz, and is related to  
236 both the bandwidth of the seismic data and bed thickness; as a consequence, it is very  
237 sensitive to frequency-dependent amplitude variation. In our seismic analysis this attribute  
238 has proved to be very effective in highlighting and mapping the top of the Cabiúnas  
239 Formation across the entire dataset.

240 4) Relative acoustic impedance (RAI). The relative acoustic impedance (called here RAI) was  
241 proposed by Chopra et al. (2009) and is the result of a simple integration of the complex  
242 trace. To calculate it first we invert the seismic amplitudes into a reflectivity series using  
243 spectral inversion. Then we transform this reflectivity series into a relative impedance  
244 layers. This step is a trace-by-trace calculation process. It basically represents the  
245 approximation of the relative acoustic impedance at high frequency components. In our

246 study it was extremely effective in highlighting the seismic textures of the various subunits  
247 recognized and mapped within the Lagoa Feia Group.

## 248 **4.2 Structural validation**

249 Low resolution and frequency of the seismic expression of the Cabiúnas and above Lagoa Feia  
250 formations, coupled with the lack of robust well constraints across these pre-rift and early syn-rift  
251 deposits, has posed significant challenges during seismic mapping. Following the seismic interpretation  
252 of these pre-salt intervals using available well and core data, several half graben structures within the  
253 top-Cabiúnas and lower Lagoa Feia group were identified, the geometries of which are controlled by  
254 the listric bounding fault (Fig. 4a, Fault 3) and a number E-dipping normal faults (Fig. 5a, Fault set 2).  
255 To test the validity of fault and the horizon identification during seismic interpretation, and in an attempt  
256 to constrain relative timings of Fault 3 and Fault set 2, a simple kinematic restoration technique was  
257 applied to this pre salt interval of the seismic line. This was performed using a simple line-length  
258 balance technique (Dahlstrom, 1969; Gibbs, 1984), with respect to seismically imaged extensional  
259 settings, of the top Cabiunas (red dotted in Fig. 5a). Given the low resolution and frequency of the  
260 seismic expression, and consequent paucity of clear stratal terminations within this part of the  
261 succession, no attempt was made to define geometries within the tilted fault blocks. Thus, two simple  
262 scenarios were used for comparison: (1) Fault Set 2 pre-exists the large listric fault (Fault 3), and is  
263 related to an early rifting phase affecting the Cabiúnas Fm and underlying deposits (Fig. 13). (2) Fault  
264 Set 2 and Fault 3 were kinematically linked during rifting, with Fault Set 2 representing a listric counter-  
265 fan along a floor fault (*sensu* Gibbs, 1984), related to offset along Fault 3 (Fig. 13).

## 266 **5. Results**

267 We will firstly focus on the characterization of the regional seismic sequence, and then concentrate on  
268 the recognition and interpretation of the main seismic facies by combining a detailed amplitude seismic  
269 mapping, image processing techniques and well bore analysis. Finally using a constant line-length  
270 approach, some kinematic models fitting the observed geometry and seismic stratigraphy are proposed  
271 and discussed.

### 272 **5.1 Seismic sequence stratigraphy surfaces.**

273 The first approach of our seismic characterization consisted of distinguishing the main regional seismic  
274 surfaces, with the aim of mapping the major seismic units using reflection terminations and sequence  
275 stratigraphic principles. Here we refer the seismic interpretation of the main seismic units with respect  
276 to the main rift faults observed. Therefore we simplify the conceptual interpretation by referring our  
277 seismic interpretation to the observed fault rift related structures even if we are aware that at regional  
278 scale some of the main pre salt units unaffected by faults (traditionally interpreted as sag units) may  
279 still comprise part of the syn-rift supersequence controlled by lower crust extension (see Karner &  
280 Gamboa, 2007 for an extended discussion). A discussion and integration of the various seismic



281 stratigraphic units and a chronostratigraphic chart of the basin locally utilized here for the Campos Basin  
282 has been presented elsewhere (Ene et al., 2015; Goldberg et al., 2017). Here we paid specific attention  
283 to the pre-salt rift basin deposits and their relation to the main rift structure by subdividing the  
284 stratigraphy into genetically related units – systems tracts, as originally defined by Brown & Fischer  
285 (1977) but following the methodology proposed in the North Sea by Prosser (1993). The main seismic  
286 units and related surfaces that have been recognized and mapped are the following (Figs. 1, 4a to d and  
287 8):

288- **Pre-rift Unit**: This is the deepest seismic unit of the framework. It consists of Pre-Cambrian plutonic  
289 and metamorphic rocks. The seismic reconnaissance of the pre-rift unconformity is precluded due to  
290 (1) its deep occurrence (over 8km), and (2) low acoustic impedance contrast between these crystalline  
291 basement rocks and the basalts of the syn-rift section and their low frequency characteristic. The main  
292 driving information are the well core and log information used to tie and calibrate the main seismic  
293 units and response to the sweetness attributes. Here we will refer to three main seismic sections named  
294 A and B and C and to three main wells here referred to as well A, B and C all located in Fig 1.

295- **Top Cabiúnas Formation**: This represents a lithological contrast between the basalts and the overlying  
296 sediments, with no time significance. The well data (the purple unit in wells B in Figs. 5b, well C in  
297 figure 5c and well A in Fig 9) characterize the Cabiúnas Formation as sediments inter-fingered with  
298 thin basalt sills. Using the well tie information, the Top Cabiúnas Formation has been mapped and  
299 defined by a very discontinuous reflection represented as a red dotted reflector in figures 5, 8 and 9.  
300 This unit is only clearly mappable by using the wells and a combination of amplitude- and frequency-  
301 dependent attributes such as the sweetness (Fig 4) that helped to enhance the very low impedance  
302 reflection. The reflection doesn't show any real lateral continuity, suggesting heterogeneity at the base  
303 of the overlying sedimentary unit. As shown in all the seismic lines (Figs 5, 8 and 9), the seismic  
304 interpreted Top Cabiúnas Formation (red dotted reflector) is intensely dissected by the extensional  
305 faults associated with the initiation of rifting.

306- **Syn-rift unit**. On top of the Top Cabiúnas Formation a thick syn-rift unit characterized internally by  
307 two main discontinuities has been systematically mapped and recognized in the sub-salt rift basin. The  
308 base of this unit is defined by the top of the Cabiúnas Formation, while the top of the entire unit is  
309 defined by a *pre salt Unconformity (base sag?)* (reflection highlighted in red in Figs. 5a,b and c), which  
310 consists of an intense erosional truncation observed across the entire rift basin which is probably locally  
311 equivalent to the pre Alagoas transitional megasequence (Guardado et al, 1990; Karner, 2000). The real  
312 significance of this unconformity will be further investigated and questioned in the following paragraph.  
313 As stated above, this syn-rift unit has been subdivided into three additional sub-units using internal  
314 reflection termination and geometry.

315- **Subunit 1**: Following the terminology by Prosser (1993) we refer to the first unit as the *Rift Initiation*  
316 *Systems Tract*, which is stratigraphically comprised between the top Cabiúnas volcanics and the first

317 lower lateral thickening reflection of the Lagoa Feia called *Half graben development surface* and  
318 mapped as a dotted orange reflector. The reflectors characterizing this subunit are very difficult to  
319 interpret due to their low resolution and poor contrast of impedance. However some characteristic  
320 reflector terminations can still be observed and help to understand the initial rift depositional history  
321 respect to the small scale rift fault. As shown in figure 5b the reflections below the *Half graben*  
322 *development surface* shows the following characteristics :

323- a) the reflectors (arrow 1, sub section 1) are parallel slightly diverging / conformable to the top Cabiunas  
324 but onlap the faults.

325- b) Within some of the internal small rift half graben the first reflector above the top Cabiúnas (arrows  
326 2 in figures 5) show a slightly fan thickening relation with some of the rift faults. The reflection  
327 termination against the faults are unclear or chaotic (Sub section 2)

328- c) very low amplitude and lateral continuity with a conformable parallel reflector geometry to the top  
329 cabiunas , but dissected by the faults (arrows 3, Sub section 3).

330- Those three type of reflector terminations have been recognized and indicated on the seismic line B  
331 (Fig 5b) and A (Fig 5c).

332- Above those generally comfortable reflectors (part of the *rift initiation tectonic system tract*) is the *Half-*  
333 *Graben Development Surface*. This surface (orange reflector in the seismic line shown in Figures 5) is  
334 characterized by a discontinuous reflector with low amplitude and parallel wavy orientation that slightly  
335 onlap the large listric fault. Here it is interpreted as syn-tectonic with respect to both the minor and  
336 certainly to the main listric fault arrays associated with the rift system and, occasionally it shows a  
337 lateral thickening towards the faults.

338- **Subunit 2:** Above the Half-Graben Development Surface is the *High Tectonic Activity Systems Tract*  
339 (sensu Prosser, 1993). This second subunit represents the principal syn-depositional half-graben  
340 structural pattern expressed as a clear lateral thickening with respect to the main large listric fault, with  
341 an intense divergent reflection pattern along the half-graben structures. It is equivalent to the mid-rift  
342 climax system tract defined by Prosser (1993). At the top of the *High Tectonic Activity Systems Tract*  
343 it is possible to define a second important regional surface called here the *Tectonic Change Surface*  
344 (mapped in blue across the seismic lines in Figs. 5a and b and c). This surface is regionally developed  
345 across the entire Campos Basin defining a clear erosional truncation that separates the *High Tectonic*  
346 *Activity Systems Tract* below from the *Low Tectonic Activity Systems Tract* above. It can represent the  
347 transition to a late rift climax system right before the cessation of the fault activity marking the post rift  
348 or sag system tract. Part of these units (as the lower units) are clearly affected by late syn - rift faults  
349 with an eastward vergence and clear higher dipping angle.

350- **Subunit 3:** the *Low Tectonic Activity Systems Tract* represents the top of the syn-rift unit and is  
351 characterized by a decrease in the divergence of the depositional reflectors, with dominance of wavy  
352 and parallel reflections, and lower displacement of the border faults, indicating a reduction in tectonic  
353 activity. It is equivalent to the late rift climax system tract of Prosser (1993). A third regional surface

354 called the *pre salt base Unconformity* (in red in Figs. 5 and 8 and 9) defines the top of the subunit *Low*  
355 *Tectonic Activity System Tract*, now characterized by horizontal versus slightly divergent reflectors.  
356 The Pre salt base unconformity is represented by an intense erosional truncation observed and mappable  
357 across the entire basin analysed. As clearly indicated in Fig 5c, outside the mini syn-rift basin bordered  
358 by the main syn rift fault system, subunits 1 and 2 are strongly reduced between the top Cabiúnas  
359 Formation and the *pre salt base unconformity*.

#### 360 **Pre salt late-syn rift unconformity:**

361 In our seismic dataset above the post rift unconformity (Red) and below the base of the salt (green) we  
362 observe an un-faulted seismic unit characterized by sub-parallel reflector capping the clear brittle  
363 faulted syn rift depocenters. This pre salt unit is characterized by wavy and discontinuous reflections  
364 with synformal structures strongly influenced by the base of the salt. No visible fault is affecting the  
365 unit that seems conformable (with no lateral thickening) onto the previous low tectonic activity system  
366 track. This unit overfills and extends beyond the margins of the previous rift structures (Fig 5c), The  
367 top surface is mapped as a green reflector (Figs. 5 and 8) and represents the base of the salt. This top  
368 surface appear as an unconformity equivalent to the *post rift system tract* sensu Prosser (1983) or to an  
369 intermediate stage devoid of visible fault structure leading to a *post rift system tract*.

#### 370 **5.2 Structural setting and major system tracts**

371 The Lagoa Feia Group in the Campos Basin is associated with basement-involved block rotation  
372 faulting on a subsiding crust, with widespread mafic volcanism between 111 and 134 Ma (Amaral et  
373 al., 1966; Cordani et al., 1972; Mizusaki et al., 1988). As shown in the large seismic section in Fig. 5c  
374 the pre-salt units are mainly characterized by a series of normal faults associated with an early rift stage,  
375 alternating with half-grabens where the main boundary fault develops, probably relatively late in the  
376 basin evolution, and which affects both the high tectonic activity system tract and low tectonic activity  
377 system tract. A closer look at the overall normal faults (with red numerations in figure 5 a, b and c) is  
378 proposed through the figure 5a and 6b representing the seismic line named B and A in figure 1. The  
379 reader should note that their represented geometry is here biased by the vertical exaggeration here 1.5:1.

380 In figure 5a a complete section of one of the half grabens is shown with a low vertical exaggeration (x  
381 1.5, for all the section 5 a to c). The half graben structure is controlled by three different oriented fault  
382 systems: low angle, small displacement normal fault (fault 2) affecting the base of the Lagoa Feia and  
383 the top cabiunas formations; high angle fault with an antithetic orientation (fault 1) with respect to the  
384 low angle faults and the large-offset listric fault (3) which controls the main graben geometry. Timing  
385 of fault populations will be further investigated through a restoration model (section in Fig 13) but the  
386 geometry and the relationship with the stratigraphy indicate that the three different fault systems were  
387 all active during the half graben structuration. The fault system 1 appears to cross most of the Lagoa  
388 Feia formation both in figures 5a to c, confirming the syn rift nature of this depositional unit, and appear

389 to have been active for longer and probably represents a later stage with respect to the fault system 2;  
390 the low angle fault (fault 2) localized in the low part of the Lagoa Feia appear to have been the triggering  
391 structure of the first rift structuration. While in some cases the main stratigraphy seems to have a clear  
392 onlapping relation with those faults while in other cases (arrow 1 figure 5b ) the lower Lagoa Feia units  
393 do not have reflector terminations with a clear relationship. The later listric fault (fault 3) clearly  
394 controls and defines the main geometry and space of the half graben and certainly affects the lateral  
395 thickening observed which is bound by the maximum rifting surface. This suggests that intermittently  
396 the listric fault has been active for a long time and that most of the deposition of the pre salt unit included  
397 the late *Low Tectonic Activity Systems Tract*.

398 Therefore From a stratigraphical point of view (refer to Fig. 2) the Lagoa Feia subunits have been  
399 structurally interpreted following the criteria and scheme proposed by Prosser (1993) and Norverdt et  
400 al. (1995):

401 The *Rift Initiation Systems Tract*, onlapping both small normal block faults (system 2, involving mostly  
402 the basement units) and the large listric fault structures (system 3) controlling most of the tectonic  
403 subsidence; In a rift related linked depositional system, those succession roughly correspond to the rift  
404 initiation starting with an early syn rift unconformity sensu Prosser (1993) and Norverdt et al (1995).

405- The *High Tectonic Activity Systems Tract* (in blue) showing an aggradation and then draping the Rift  
406 Initiation Systems Tract but laterally onlapping the main boundary faults (system 3) or the product of  
407 the scarp degradation, but still confined within individual half-graben systems. They clearly represent  
408 the early and later onset of the rift climax where subsidence controlled by the fault activities is still  
409 faster than the sedimentation. As a consequence those units are comparable with what Prosser (1993)  
410 calls the units sequence of early - mid climax syn rift and are certainly part of the syn rift megasequence  
411 of Winter (2007).

412- The *Low Tectonic Activity System Tract*, again draping and transgressing the previous unit and still  
413 onlapping (in places) the large boundary faults across the small half-graben at a more regional scale. It  
414 is bounded at the bottom by the *tectonic change surface (blue line)* that represents the late rift climax  
415 (sensu Prosser, 1993) where the listric fault activity start to decelerate leading to the first immediate  
416 post rift succession through an intermediate late *pre salt syn-rift unconformity*.

417

### 418 **5.3 Characterization of the seismic facies**

419 The main seismic interpretation and seismic image analysis consisted in recognizing the seismic facies  
420 that are repeatedly observed within he various system tract observed and recognized. The seismic facies  
421 is here defined through a combination of reflector geometry (using both continuity and reflection  
422 termination), waveform properties as the five seismic attributes appearance described so far (table in  
423 Figure 4). Specifically the use of the cosine of the phase, combined with the usual mapping of the

424 reflection terminations, proved very useful and efficient in highlighting both the thin bed, and the  
425 continuity between various reflectors. To further fine-tune the internal facies we also extracted seismic  
426 attributes related to the relative amplitude and contrast of impedance, such as the reflection strength and  
427 RAI. We then linked the various facies to their position within the fault related sub-basin to predict the  
428 environments of deposition that controlled the types of deposits (e.g. to differentiate carbonates from  
429 sandstones and mudstone units).

430 Seismic facies 1: this seismic facies is defined by chaotic and/or low amplitude reflectors (Figure 6),  
431 with no clear internal stratigraphy, often inferred to be strongly damaged by small faults and fractures.  
432 The seismic package characterized by this facies is observed mostly across the syn-rift units and is  
433 systematically juxtaposed to fault planes.

434 Seismic facies 2: This seismic facies show a facies (see Figure 6) characterized by thinly layered, semi-  
435 continuous strong to medium amplitude reflections. This facies is best observed through the RAI  
436 attributes (fig. 7) that enhance the discontinuous character as it has a granular and dotted signal in clear  
437 contrast with the surrounding facies 3. The cosine of phase expression of the texture confines the thin  
438 and non-continuous phase character of the reflectors (Figure 7b). This seismic facies is systematically  
439 observed across the all syn-rift units (high to low system tract), and characterizes the package with an  
440 onlapping and slightly lateral thickening geometry.

441 Seismic facies 3. This seismic facies is observed throughout the Lagoa Feia unit from the syn rift to the  
442 high and low system tract sub units scattered across the half graben basin. It is characterized by very  
443 continuous, thick and strong reflections, interbedded with or even floating within the thinly-layered  
444 seismic package (seismic facies 2). The seismic character is clearly represented by the RAI attributes,  
445 highlighting strong continuous and bright reflectors (Fig. 7a). Similarly the cosine of phase shows quite  
446 thick and continuous reflectors (figure 7b). The packages show quite abrupt boundaries, but do not show  
447 any onlap or lateral thickening. They appear as the brightest and distinctive reflectors of the pre-salt  
448 units.

449 Seismic facies 4. A fourth seismic facies (Fig. 6) is characterized by a wipe-out zone where the seismic  
450 reflections are strongly disrupted, affected by low amplitude, and pull-ups typical of intrusive features.  
451 This seismic character crosses all of the Lagoa Feia connecting the Cabiúnas Formation, reaching the  
452 base of the Sag units, suggesting a late/post depositional event with respect to rifting. For an extensive  
453 analysis and discussion of those feature we refer to Alvarenga et al (2016).

454 The seismic facies recognized has been then mapped across the seismic lines B,C and A using the  
455 proposed classification (Figs 6 and 7) and the results are shown respectively in Figures 8, 9 and 10  
456 (the numbers 1 to 3 represent the seismic facies described above). The dotted lines represent the  
457 boundaries of seismic facies 3.

#### 458 **5.4 Constraints from the well data**

459 Image analysis of individual units recognized through their facies response can potentially improve our  
460 understanding of the volumetric distribution of the various lithological units, and prepare the ground  
461 for future reservoir characterization and seismic facies analysis of the sub-salt Lagoa Feia units. Brown  
462 & Fisher (1980) defined seismic facies as the expression on seismic reflections of geological factors  
463 that generate them, such as lithology, stratification, depositional features, etc. In this case although we  
464 are lacking a robust lithological calibration of seismic facies we matched the seismic facies with the  
465 two available wells (called here well A and well B) after time-converting them using checkshots  
466 information. These two well data represented the only geological and petrophysical constraints  
467 available in the mapping area. They have been part of the dataset used to define the main petrography  
468 and sedimentology background by Armelenti et al (2016) and Goldberg et al (2017). Their location and  
469 relative position respect to the seismic line proposed for this studies are indicated in figure 1. We first  
470 briefly describe below the main stratigraphical information obtained from the two wells (Fig 11 for a  
471 description), and then use it to define the main seismic units matching the seismic facies mapping  
472 analysis.

473 As shown in Figures 8 to 10, wireline log data and continuous core information from two wells (well A  
474 and B) have been used to assess the seismic textures recognized within the Lagoa Feia, and assign them  
475 a geological significance. A legend describing the main lithological units representation is proposed in  
476 figure 11 using the Well B (Fig 11). The following main lithological units have been recognized:  
477 conglomerate (orange); sandstone (red); layered limestones (calcarenite, light blue and calcilutite pale  
478 blue) and coquina (dark blue) shale and shaly sandstone (green); and marl/mudstone (grey) units. In  
479 yellow are represented the sandstone observed within and above the salt unit (Figs 8 and 9). The basalts  
480 in the Cabiúnas Formation are marked by the purple colour (Figs 8-10). A detailed petrographical,  
481 petrological and sedimentological description of these cores is given by Armalenti et al. (2016) and  
482 Goldberg et al. (2017). Here we use only the main lithologies for calibration purposes, to constrain and  
483 interpret the main seismic facies. The Well A (Fig 8) extends to some distance below the salt, and  
484 penetrates the pre- and syn-rift deposits. The well B is instead represented in figures 9 and 10. The  
485 section crossing the main facies 2 and 3 has been zoomed in Fig 11.

486 Well A (Figure 8) tying seismic line C: well A shows three main package of unit part of the high and  
487 low stand system tract. A first package between the maximum rifting surface (top High tectonic activity  
488 system track) and the post rift unconformity characterized by semi-continuous, thinly layered  
489 reflections of low amplitude defined by a complex alternation of thick units of sandstone and  
490 shale/mudstone the seismic facies correspond to the seismic texture described as 1. A second package  
491 placed within the High tectonic system track ) and characterized by a strong correspondence of the “fat  
492 and bright” reflectors (described as seismic facies 2) matching with the occurrence of very finely layered  
493 units characterized by alternation of coarse-grained limestones, calcilutite with mudstone / shale and

494 the Coquinas unit (see the yellow brackets indicating the limestone units). A third package bounded  
495 between the *high system track* and the Cabiúnas formation (but mostly within the *Rift initiation system*  
496 *track*) is characterized by similar semi-continuous, thinly layered reflections of low amplitude as the  
497 first package. This package is characterized instead by an alternance of thick conglomerate unit with  
498 shale units and thin layer calcarenite. This seems to suggest that the bright and thick reflections are  
499 associated with the presence of coarse-grained limestones within the Lagoa Feia Group.

500 Well B (Figures 9, 10 and magnified version in Figure 11) tying seismic lines B and A: this well  
501 penetrates through the Lagoa Feia Group depositional units at a more distal position respect to the large  
502 scale listric fault. This unit is slightly more condensed and the bottom part slightly penetrates the  
503 Cabiúnas Formation. Again a similar sequence of packages (from top to bottom) can be recognized. A  
504 first package located mostly in the low system track (above the *maximum rifting surface*) characterized  
505 by a seismic facies of the type 2 tying mostly an alternation of thick units of sandstone and  
506 shale/mudstone. A second package defined mostly by a seismic facies of type 3 mostly confined within  
507 the High tectonic system track and the low system track characterized by alternation of coarse-grained  
508 limestones, calcutite with mudstone / shale and the Coquinas unit. A third package is extremely  
509 similar to what has been described with the well A where seismic expression is defined mostly by the  
510 seismic facies 2 characterized by the alternance of thick shale, conglomerate units and thiny calcarenite,  
511 Therefore well B confirms similar relations described by the well A, where the presence of dense  
512 coquinas and calcarenite is clearly marked by fat and bright reflections associated with seismic facies  
513 3 across the entire unit. In both case the basalts (in the pre/syn rift units) of the Cabiúnas Formation do  
514 not generate any real contrast of impedance, possibly due to the absorption effect of the high frequency  
515 component of the signal of the above layered limestone subunits.

516 None of the two wells adds any information about the seismic facies 1, as they do not intersect the  
517 associated unit. However the following seismic consideration can help to recognize and assign a clear  
518 relationship of the seismic texture to the chaotic and conglomeratic deposit bordering the main faults.  
519 All the seismic sections imaging the deep rift structure represented in Figures 8, 9 and 10 indicate that  
520 the chaotic and low amplitude seismic texture without any internal stratigraphy recognized here as  
521 seismic texture 1 area systematically juxtaposed to small or large fault bordering the small sub-basin  
522 underlying the sag and salt unit.

523 The unit shows also marked amplitude discontinuity, often intersected by small faults, producing a  
524 dotted signature of the signal. The seismic character, location and geometry all suggest the deposit may  
525 be related to a range of hanging-wall collapse mechanisms. Collapse of the hanging-wall to the main  
526 listric fault (Fault 3) may be attributed to listric fan formation during extensional faulting (Gibbs, 1984)  
527 and associated rock fall, debris flow and sediment slumping processes (Prosser,1993). Similarly,  
528 recurrent extensional pulses along this border fault may have remobilized shallow-water sediments and  
529 allowed gravitational mixing and re-deposition of both pre-rift footwall and syn-rift hanging-wall

530 material (Goldberg et al., 2017). Figure 12 shows a small fault-related basin imaged by the seismic line  
531 A and characterized by the Lagoa Feia infilling, in which the seismic facies proposed above have been  
532 recognized and mapped out. From what observed the two seismic facies 2 and 3 seem to both  
533 characterize the Atafona Formation and they consist of siltstones, sandstones and lacustrine shales with  
534 a distinctive talc-stevensite mineralogy, interbedded thin lacustrine limestones (for a detailed  
535 sedimentological analysis see Goldberg et al., 2017)

## 536 **5.5 Structural considerations and kinematic restoration test**

537 Large-scale seismic mapping of the Lagoa Feia Formation (across the seismic lines A,B and C) allowed  
538 for a clear description of their stratigraphic relationship with the syn-rift faults. All of the structures and  
539 reflection terminations observed (Figs 5) suggest that the Lagoa Feia Formation was deposited during  
540 tectonic extension, when certainly faults populations 2 and 3 were active and displacing (Figs. 5a and  
541 5b). Cross-cutting relationships also show that the W-dipping faults in the western parts of Lines A and  
542 B (Fault Set 1) post-dating the deposition of the upper part (*high to low tectonic system tract*) of the  
543 Lagoa Feia Fm and thus suggest a stage of extension that post-dates that of faults set 2 and Fault set 3.  
544 Seismic mapping of the Top Cabiúnas and its relation with the extensional faults in the lower part of  
545 the *rift initiation system track* however, does not provide an obvious relative timing between the Fault  
546 Set 2 and Fault set 3 - whether movement on these faults were synchronous or one population pre-dated  
547 the other. Therefore a simple restoration approach applied to Seismic Line A, which retains line lengths  
548 of key reflectors (Fig. 13), provides some first approximations and simple observations that help to  
549 clarify some of these aspects. Two scenarios have been investigated. A Scenario 1 (Fig. 13 a to d) in  
550 which the E-dipping faults are kinematically linked and coeval to the large listric fault. A scenario 2  
551 (Fig. 13 ), in which E-dipping normal faults which deform the base of the Lagoa Feia Formation, the  
552 Cabiúnas Formation, and underlying deposits, before the onset of fault movement along the large W-  
553 dipping listric fault. Both scenarios, when restored, produce very similar results and in both cases a final  
554 restorable structure similar to those mapped in Seismic Line A (Fig. 13d). Essentially the following  
555 kinematic evolution can be proposed:

556 An initial extensional rift event where the low angle small rift fault are active and create the small rift  
557 structure with syn depositional structure which geometry and architecture correspond to the *Rift*  
558 *initiation system track* (Fig 13 b). At a certain point the stress field condition produces some strain  
559 localization where one of the small west dipping faults start to localize the extension (Figs. 13 c to d)  
560 producing a large listric fault (Fig. 13d) that will control the main half graben structure. That listric  
561 fault will produce the main conglomerate breccia and reworked deposit observed in all the seismic lines  
562 (Figs. 8 , 9 and 10) and described as seismic facies 1 (Fig. 6) . The system will continue till the extension  
563 will relax or decelerate or till the stress field will re orient activating new extensional fault population  
564 aside of the main basin (Fig. 13 e).



565 Due to poor resolution and the degraded nature of the seismic data, particularly in the hanging-wall to  
566 Fault 3 (Seismic Facies 1), and in the lower part of the Lagoa Feia Formation (Seismic Facies 2),  
567 refinement of structural models, and a determination of relative fault timings (of Fault Set 2 and fault  
568 3) has not been possible. Therefore two problems still remain of limited solutions:

569 Bedding geometries (and their reflector terminations) of syn-rift deposits in the initial units of the Lagoa  
570 Feia Formation are poorly constrained and thus do not provide a definitive solution to relative fault  
571 timings. The lack of clearly defined seismic horizons in the hanging-wall of Fault 3, particularly  
572 adjacent to the fault, does not allow for estimates of syn-rift deposition rates.

573 Similarly, the presence of listric fault roll-overs or synthetic fans cannot be deduced from the available  
574 data (Gibbs, 1983). Thus, the nature of the seismic expression does not provide sufficient data for robust  
575 kinematic restoration and a definitive relative timing for Fault Set 2 and Fault 3 but clearly does not  
576 exclude kinematically their mutual activities.

577 Finally the age of or nature of the main low angle fault have not been resolved either as the restoration  
578 does not rule out the possibility that part of those initial faults were not inherited from previous  
579 structural history (Fig 5b, zoomed example 1 where the reflector seem to onlap the structure)

580

## 581 **6. Discussion**

### 582 **6.1 Facies interpretation**

583 The workflow and seismic characterization proposed here allowed us to map and reconstruct the main  
584 pre salt units structure and interpret the seismic facies of some of the major units of the lower Lagoa  
585 Feia Group. Due to the particular position of the lower Lagoa Feia, sandwiched between the salt unit  
586 above and the basalt below, in a present-day deep water location, the quality of the seismic data over  
587 the main sequence and sub-units is very noisy and the resolution is limited producing a lot of  
588 uncertainty. Most of the high frequencies are in fact absorbed by the salt and partly by the main  
589 calcarenite, calcilutite and coquinas-limestone units (Fig 3a). Moreover the seismic properties observed  
590 indicate the pre/syn-rift units constituted by basalt and interlayered shale (Cabiúnas Formation and  
591 lower portion of the Lagoa Feia Group) are rendered almost invisible, or characterized by very weak  
592 reflections. The basaltic units are in fact inferred mainly through well bore and well log information but  
593 cannot be traced out through a clear amplitude seismic distinctive response. This could suggest that  
594 within the Cabiúnas Formation the thin bed character of the interlayered basaltic intrusion is probably  
595 producing an extremely damaged or poor signal, certainly hiding more complex relationships than  
596 simple layering structure as various other authors has suggested (Magee et al.,2015).

597 As a consequence our attention has been here focused on the above seismic package part of the *rift*  
598 *initiation tract, high and low tectonic system tract* and the post rift units above the Cabiúnas Formation.

599 Using limited well log and core information to calibrate their seismic waveform properties three major  
600 seismic facies have been recognized and associated with three different lithological units characterizing  
601 the Lagoa Feia Group (Figure 9).

6021) The units associated with seismic facies 1 show chaotic reflectors, without continuity (see the area  
603 enclosed by the blue line in Figs 11 and 12) and with low average amplitude. Its occurrence is  
604 geographically associated with the border faults, suggesting that their deposition is controlled by the  
605 fault movement (Figs 11 and 12). This facies seems never to occur within the earliest syn-rift deposit,  
606 probably because there was insufficient topographic relief at this time to form the deposit. The same  
607 applies to the top units of the basin (as observed in seismic line in figures 8 and 9), where this seismic  
608 facies seems not to occur, probably because during the late its later stages of development the basin was  
609 already starting to behave as a post rift with low fault related subsidence. As a consequence, this facies  
610 is interpreted as breccia and re depositional slope deposits originated from erosive mechanism along  
611 the fault edge due to the displacement increase of the footwall block right after its failure. They are  
612 commonly interpreted as conglomeratic deposits, named as border-fault deposits (Goldberg et al, 2017).  
613 Seismic facies 2 shows instead a diverging configuration across the majority of the sub-basin analyzed,  
614 suggesting a hummocky configuration in the depocenter across all the half-grabens examined (Figures  
615 8 and 9). The shale/marl and thick sandstone units that compose the facies unit 2 are characterized by  
616 the absence of coquinas or other carbonates. They affect both unit from the *initial rift system tract* as  
617 much as the upper part of the *High tectonic system tract* and the *low system tract*. This facies is rather  
618 characterized and controlled by the thick layered and low amplitude continuous reflectors (Figs 5 and  
619 6) rather than the compositional component (within which the bright thick units of seismic facies 3 are  
620 embedded). According to the well data, and to the existing petrographical information (Armelenti et al.,  
621 2016; Goldberg et al., 2017), facies 2 can be linked both to the Barremian aged Atafona Formation  
622 consisting of siltstones, sandstones and lacustrine shales with a distinctive talc-stevensite mineralogy,  
623 interbedded thin lacustrine limestones as to the Itabapoana Formation (alluvial fans/fan deltas  
624 proximally and lacustrine/lagoonal sediments distally) and also of Barremian to lower Aptian age, partly  
625 laterally equivalent to Atafona. The two units has been interpreted By Goldberg et al. (2017) as fine-  
626 grained lake sediments, associated with sediment gravity flow deposits.

6272) Seismic facies 3 shows reflections with a rather parallel configuration, but with an average high  
628 amplitude and good continuity, producing a rather tabular geometry (Figs 5 and 6). As shown in Figure  
629 5 they show the highest frequency response within the High and low tectonic system tract and the. The  
630 reflector terminations seem to indicate onlap geometry characterized also by some structural truncation.  
631 The facies 3 is usually dispersed or sandwiched within the facies 2 (Atafona and Itabaquana formations)  
632 , and can occur both along the basin margins as well as in the depocenter of half-grabens (Figs 8, 9 and  
633 10). This facies has been interpreted, using the existing well log information and petrographical  
634 information (Armelenti et al. 2015; Goldberg et al.,2016), as rudstone/grainstone carbonate units, which

635 are locally arranged in the form of mounds, and laterally shading into texture 2. Some authors such as  
636 Abrahão & Warme (1990) and Rangel & Carminatti (2000) state that the deposits of thick carbonate  
637 can be interpreted as shallow marine deposits. However, due to its scattered location, texture 3 is here  
638 interpreted as a result of reworking and erosion of a shallow bank. The deposits associated with this  
639 seismic facies have been here named as coarse grain-dominated re-sedimented deposits (Goldberg et  
640 al.,2017).

641 A fourth seismic facies shown in Figure 8 indicates an intrusive feature, characterized by a large wipe-  
642 out zones with some pull-up velocity effects enhanced (possibly exaggerated by an incorrect velocity  
643 model) affecting the entire Lagoa Feia Group and touching the sag unit. This feature has not previously  
644 been described, but its geometry and texture suggest that important gas chimneys affect the entire pre-  
645 salt unit. The nature and significance of this structure has been extensively described in the companion  
646 paper by Alvarenga et al (2016)

## 647 **6.2 Structural evolution**

648 The simple kinematic test coupled to the seismic mapping across three seismic line A to C (driven by  
649 the three well data analysis) helped us to reframe and define the structural characteristic of the Campos  
650 pre salt structure in the area of investigation. The rifted half graben basin where most of the re-  
651 depositional system has been described and here investigate show a story characterized by west dipping  
652 low angle fault initially triggering the main extension , affecting the top Cabiúnas Formation and  
653 creating the initial space for the first Lagoa Feia unit (Fig 13 a to c). Those fault seem to remain active  
654 during the enucleation and main displacement activity of the large lystric fault (Fig 13 d to e) that will  
655 shape the final half graben structure and allow for the major unit of the Laoga feia to be deposited and  
656 preserved so far. During the deposition of the mid-upper unit of the Lagoa Feia (High to low syn rift  
657 deposition system tract) the rift system seem to still be active and probably affected by a different stress  
658 orientation that re activate or enucleate east dipping fault (fault system 3 in fig 5a and Fig 13 d). Those  
659 two fault systems will contribute to createthe syncline type half graben system observed across the  
660 Campos Basin. Different cross section, represented in Fig 14, seem to confirm that trend and that overall  
661 geometry: from the different seismic line crossing along the extension (Fig 14, section 1 2 and 4) and  
662 orthogonally to it (3 in Fig 14) they all show that the pre salt Lagoa Feia unit (rift initiation, High and  
663 low rift system) has been deposited and controlled by the large listric fault and some of the out of  
664 sequence extensional late fault. As suggested by some reflection termination (Fig 5d) there is no reason  
665 to rule out the possibility that some of the initial low angle faults may have been in reality part of a pre-  
666 existing inherited structure affecting the Cabiúnas Formation, re activated during the main rifting  
667 activity. Overall the framework seems to suggest a long lived extensional system affected by several  
668 low angle and listric faults which in some cases were re activated during the final subsidence history.  
669 The lateral thickening but also onlapping through an interfingered relationship with the border fault  
670 deposit, suggested that the Lagoa Feia unit is a syn rift depositional unit. In that case they should not be

671 assigned to the post rift supersequence as originally suggested by Winter et al. (2007). Finally the faults  
672 do not affect the pre salt unit confined between the pre salt syn rift unconformity and the base salt but  
673 there are no obvious relation to rule out the possibility that this unit may still be affected by a syn rift  
674 activity driven by a deep crustal extension devoid of visible upper fault.

675

### 676 **6.3 Pre salt late-syn rift unconformity: Sag unit?**

677 From our mapping the Lagoa Feia Group is covered by the transitional late Syn-Rift pre salt sequence  
678 bounded here by the *pre salt unconformity* (red units), observed at a regional scale (see sections in  
679 figures 5) and characterized by a phase where the differential subsidence across the fault plane ceases.  
680 In this paper we restrict the analysis of our observation to a specific single half graben system. Moreover  
681 the lack of informations from the well bore doesn't allow us to further investigate the nature of this post  
682 rift unconformity unit with respect to the regional tectonic of the passive margin. Within our area of  
683 investigation the lack of upper crustal rift deformation in our seismic sections (Figs 5 and 8) can't rule  
684 out the possibility that this Pre salt late-syn rift unit was still subsiding under the depth-dependent  
685 extension (Karner & Gamboa, 2007) determined by the rate of crustal extension. Therefore we cannot  
686 exclude that this late syn rift unit could be related to the last crustal adjustments before the continental  
687 effective break-up (as predicted by Wernicke, 1985). A similar interpretation would then place this unit  
688 as structurally linked to the deformation transition from fault-controlled brittle deformation to depth-  
689 dependent lithospheric thinning, essentially triggered by ductile stretching of the lower crust (Kusznir  
690 and Karner, 2007). Other authors instead have interpreted that unit as a Sag Unit (Guardado et al.1990;  
691 Contreras, 2010) and therefore as a sedimentary precursor of the salt units characterized by halokinetic  
692 features. In that case the pre salt late syn rift unconformity may correspond to the onset of a regional  
693 lower Aptian unconformity, termed by some authors as the pre Alagoas unconformity (Karner, 2000),  
694 which could support these units here being interpreted as a gentle sag phase part of the rift  
695 supersequence leading to the evaporate or salt sequences (Guardado et al.1990). The lack of  
696 stratigraphic constrain and ages still allows us to interpret this succession as a pre salt basin fill, involved  
697 into a continued syn-rift extension without major visible extensional faulting typical of the upper crust  
698 (Karner, 2000; Karner and Gambôa, 2007, Contrera et al., 2010). If this is the case this implies that the  
699 unconformity needs to be interpreted as pre salt base unconformity. A secondary implication is that the  
700 upper part of the Lagoa formation may not be included or interpreted as a post rift units and therefore  
701 may be considered part of the post rift supersequences by suggested by Winter et al. (2000).

702

### 703 **7 Conclusion**

704 A seismic and structural interpretation of the pre-salt Lagoa Feia Group is here proposed through the  
705 analysis of a combination of seismic and well data from the Campos Basin. Our analysis shows that:

706- - By using some basic attributes of the seismic signal it is possible to recognize some distinctive seismic  
707 facies characterizing the main lacustrine depositional environment across the entire region of the  
708 Campos Basin.

709- - The main seismic facies, calibrated through well data, can be linked to the main depositional units of  
710 the Lagoa Feia Group, characterizing border fault deposits; dominantly fine-grained re-sedimented  
711 deposits; dominantly coarse-grained, carbonate-rich re-sedimented deposits; and intrusive wipe out  
712 zones affecting the entire pre-salt unit.

713- - The seismic facies allow the description and characterization of an internal seismic architecture of the  
714 sub-basin related to the syn-rift tectonic activity, suggesting that the Lagoa Feia seismostratigraphy  
715 represents a fault-restricted lacustrine depositional environment, strongly affected by long-lived  
716 intermittent rift tectonics.

717- - Restoration models suggest that the extensional rift tectonics has been intermittent but affected by  
718 different populations of normal faults through the pre salt depositional history. All the faults likely  
719 contributed to trigger the main re depositional nature of the main lacustrine deposit but also to shape  
720 the syncline geometry of the main half graben preserving the Lagoa Feia unit.

721- - A unit here described as pre salt late rift unconformity may represent or a later syn- rift response to  
722 lithospheric deformation or a intermediate (syn- rift) sag phase precluding to the salt deposit affecting  
723 the entire campos basin.

724

725 **Acknowledgement:** The authors thank BG Brasil, a wholly owned subsidiary of Royal Dutch Shell  
726 plc, for financial support for this project and permission to publish. This work was sponsored by the  
727 BG funded Deep Rift project (BG-UFRGS-Aberdeen). The paper used Petrel (Schlumberger) and  
728 Geoteric (ffA) to interpret the seismic dataset. Constructive comments on an initial draft by T.Alves  
729 and Moriak are greatly appreciated. We thanks Brent Wignall for comments.

730

## 731 **Bibliography**

732

733 Abrahao, D., Warme, J.E. 1990. Lacustrine and associated deposits in a rifted continental margin-lower  
734 Cretaceous Lagoa Feia Formation, Campos Basin, Offshore Brazil. in Lacustrine Basin Exploration,  
735 Case Studies and Modern Analogs, Vol. 50, pp. 287–305, ed. Katz B.J., AAPG Memoir.

736

737 Amaral, G., Cordani, U. G., Kawashita, K., and Reynolds, J. H, 1966. Potassium argon dates of basaltic  
738 rocks from southern Brazil. Geochim. Cosmochim. Acta, 30:159-189.

739

740 Alvarenga, R., Iacopini, D., Kuchle, J., Scherer, C. & Goldberg, K. 2016. 'Seismic characteristics and  
741 distribution of hydrothermal vent complexes in the Cretaceous Offshore Rift Section of the Campos  
742 Basin, Offshore Brazil'. *Marine and Petroleum Geology*.

743

744 Armelenti, G., Goldberg, K., Kuchle, J., De Ros, L.F. 2016. Deposition, diagenesis and reservoir  
745 potential of non-carbonate sedimentary rocks from the rift section of Campos Basin, Brazil. *Pet.  
746 Geosci.*, 22, 223-239

747

748 Brown, L.F., Fisher, W.L., 1977. Seismic-stratigraphic interpretation of depositional systems: examples  
749 from Brazilian rift and pull-apart basins. In: PAYTON, C.E. (Ed.) *Seismic stratigraphy: applications to  
750 hydrocarbon exploration*. AAPG, Memoir 26, Tulsa, p. 213-248.

751

752 Chopra, S., Marfurt, K.J. 2007. Seismic attributes for prospect identification and reservoir  
753 characterization. SEG books.

754

755 Chopra S, Castagna J P., Xu Y. Relative acoustic impedance defines thin reservoir horizons. *Search and  
756 Discovery Article #40435* (2009)

757

758 Contrera, J., Zuhlke., Bowman., S., Bechstadt., T., (2010). Seismic stratigraphy and subsidence  
759 analysis of the southern Brazilian margin (Campos, Santos and Pelotas basins). *Marine and Petroleum  
760 Geology*. 27, 1952-1980.

761

762 Demercian S., Szatmari P., Cobbold P.R. 1993. Style and pattern of salt diapirs due to thin-skinned  
763 gravitational gliding, Campos and Santos basins, offshore Brazil. *Tectonophysics*, 228, 393-433

764

765 Colpaert, A., Pickard, N., J Mienert, j., Henriksen, L.B., Rafaelsen, b., Andreassen, K.. 2007. 3D  
766 seismic analysis of an Upper Palaeozoic Carbonate succession of the Eastern Finnmark Platform area  
767 Norwegian Barents Sea. *Sedimentary Geology*, 79-98.

768

769 Davison. 1999. Tectonics and hydrocarbon distribution along the Brazilian South Atlantic margin. In:  
770 Cameron, N. R., Bate, R. H. & Clure, V. S. (eds) *The Oil and Gas Habitats of the South Atlantic*.  
771 Geological Society, London, Special Publications, 153, 133-151

772

773 Davison, I. 2007. Geology and tectonics of the South Atlantic Brazilian salt basins. In: Reis, A. C.,  
774 Butler, R. W. H. & Graham, R. H. (eds) *Deformation of the Continental Crust: the Legacy of Mike*  
775 Coward. Geological Society, London, Special Publications, 272, 345–359.

776

777 Dahlstrom, C.D.A., 1969. Balanced cross sections. *Canadian Journal of Earth Sciences*, 6(4), pp.743-  
778 757.

779

780 De Matos. M; Osorio P., Johann, PRS. 2007. Unsupervised seismic facies analysis using wavelet  
781 transform and self-organizing maps. *Geophysics*, 72, 9-22.

782

783 Duda, R.O.,Hart, P. O., and Stork, D.G. 2001, *Pattern classification*, 2nd ed.:JohnWiley & Sons, Inc.

784

785 Gibbs, A.D., 1983. Balanced cross-section construction from seismic sections in areas of extensional  
786 tectonics. *Journal of structural geology*, 5(2), pp.153-160.

787

788 Gibbs, A.D., 1984. Structural evolution of extensional basin margins. *Journal of the Geological Society*,  
789 141(4), pp.609-620.

790

791 Goldberg, K., Kuchle,J., Scherer, S; Alvarenga, R. Ene, PL., Armelenti. G. 2017. Re-sedimented  
792 deposits in the rift section of the Campos Basin. *Marine and Petroleum Geology* 80, 412-431

793

794 Haralick, R. M., K. Shanmugam, and I. Dinstein, 1973, Textural features for image classification: *IEEE*  
795 *Transactions on Systems, Man and Cybernetics*, SMC-3, 610–621.

796

797 Hart, B.S (2008) Channel detection in 3D seismic data using sweetness,*AAPG*, 92, 733-742

798

799 Karner, G.D. (2000) Rifts of the Campos and Santos Basins, Southeastern Brazil: Distribution and  
800 Timing, AAPG Memoir 73, 301315.  
801

802 Karner, G. D. & Gamboa, L. A. P. 2007. Timing and origin of the South Atlantic pre-salt sag basins  
803 and their capping evaporates. In: Schreiber, B. C., Lugli, S. & Babel, M. (eds) *Evaporites through Space*  
804 *and Time*. Geological Society, London, Special Publications, 285, 15–35.  
805

806 Kumar, N., L. A. P. Gamboa, B. C. Schreiber, and J. Mascle (1977), Geologic history and origin of Sao  
807 Paulo Plateau (southeastern Brazilian margin), comparison with the Angolan margin, and the early  
808 evolution of the northern South Atlantic, in *Initial Reports of the Deep Sea Drilling Project*, vol. 39,  
809 edited by P. R. Supko and K. Perch-Nielsen, pp. 927–945, Texas A & M Univ., College Station, Tex.  
810

811 Magee, C., Maharaj, S.M., Wrona, T., and Jackson, C.A.L., 2015, Controls on the expression of  
812 igneous intrusions in seismic reflection data: *Geosphere*, v. 11, p. 1024–1041, doi: 10.1130/  
813 /GES01150.1  
814

815 Mohriak, W., Szatmari, P. & Anjos, S. M. C. (eds) 2008. *Salt: Geologia e Tectonica*. Beca Edicoes  
816 Ltda, Sao Paulo, Brazil.  
817

818 Mitchum Jr., R.M., Vail, P.R., Sangree, J. B., 1977. Seismic stratigraphy and global changes of sea  
819 level, Part 6: Stratigraphic interpretation of seismic reflection patterns in depositional sequences. In:  
820 Payton, C.E. (ed.). *Seismic Stratigraphy - Applications to Hydrocarbon Exploration*. Tulsa, AAPG, 117-  
821 133 (Memoir # 26).

822 Mizusaki, A.M.P., Thomaz Filho, A. Valença, J.G. 1988. VolcanoSedimentary Sequence of Neocomian  
823 age in Campos Basin (Brazil). *Revista Brasileira de Geociências*, 18:247-251.  
824

825 Mohriak, W.U., Mello, M.R., Dewey, J.F., Maxwell., J.R, 1990. Petroleum geology of the  
826 Campos Basin, offshore Brazil. *Geological Society London Special Publications* 50(1):119-  
827 141

828 Mohriak, W. U., Hobbs, r. & Dewey, J. F. . 1990. Basin-forming processes and the deep structure of the  
829 Campos Basin, offshore Brazil. *Marine and Petroleum Geology*, 7, 94–122.  
830



831 Moriak, W U, Szatamri,P. Anjos, S. 2012. Salt: geology and tectonics of selected Brazilian basins in  
832 their global context. From:Alsop, G. I.,Archer, S. G.,Hartley, A. J.,Grant, N. T.&Hodgkinson, R. (eds)  
833 2012. Salt Tectonics, Sediments and Prospectivity. Geological Society, London, Special Publications,  
834 363, 131–158.

835

836 Mohriak,W.U.,Nemčok., N and Enciso.,G. 2008. South Atlantic divergent margin evolution: rift-border  
837 uplift and salt tectonics in the basins of SE Brazil. Geological Society, London, Special Publications  
838 2008, v. 294, p. 365-398

839 Moulin, M., D. Aslanian, M. Rabineau, M. Patriat, and L. Matias (2012), Kinematic keys of the Santos-  
840 Namibe basins, in Conjugate Divergent Margins, Spec. Publ., vol. 369, edited by W. U. Mohriak et al.,  
841 Geol. Soc., London.

842 Posamentier, H., Kolla, V, Seismic Geomorphology and Stratigraphy of Depositional Elements in  
843 Deep-Water Settings 2003, Journal of Sedimentary Research,73, 367–388.

844

845 Prosser, S. Rift related linked depositional system and their seismic expression. 1993 From Williams  
846 G,D & A.Dobb, 1993. Tectonics and seismic sequence stratigraphy. Geological Society Special  
847 Publication, 71, 35-66.

848

849 Prather, B. E., J. R. Booth, G. S. Steffens, and P. A. Craig, 1998, Classification, lithologic  
850 calibration, and stratigraphic succession of seismic facies of intraslope basins, deep-water Gulf of  
851 Mexico; errata: AAPG bulletin, v. 82, p. 707R

852

853 Prather B. E., Booth J. R., Steffens G. S, and Craig P. A.. 1998. Classification, Lithologic Calibration,  
854 and Stratigraphic Succession of Seismic Facies of Intraslope Basins, Deep-Water Gulf of Mexico.  
855 AAPG Bulletin, 82, 701–728.

856

857 Radovich, B. J., and R. B. Oliveros, 1998, 3-D sequence interpretation of seismic instantaneous  
858 attributes from the Gorgon field: The Leading Edge, 17, 1286–1293.

859

860 Rangel, H.D., Martins, F.A.L., Esteves, F.R., Feijó, F.J. 1994. Bacia de Campos. Boletim de  
861 Geociências da PETROBRAS, 8:203-218.

862

863 Reed IV, T.B. and Hussong, D. 1989. Digital image processing techniques for enhancement and  
864 classification of SeaMARC II Side Scan Sonar Imagery. *Journal of Geophysical Research* 94: doi:  
865 10.1029/89JB00409. issn: 0148-0227.

866

867 Sarg J. F., James S. Schuelke. 2003. Integrated seismic analysis of carbonate reservoirs: From the  
868 framework to the volume attributes *The Leading Edge*, 2, 640-645

869

870 Stanton N., Masini, E. 2013. The rifting evolution of the Santos Basin: A Geophysical view. 13th  
871 International Congress of the Brazilian Geophysical Society & EXPOGEF, Rio de Janeiro, Brazil, 26–  
872 29 August 2013: pp. 1690-1693. [doi.org/10.1190/sbgf2013-346](https://doi.org/10.1190/sbgf2013-346))

873

874 Taner, M. T., and Sheriff, R. E., 1977, Application of amplitude, frequency, and other attributes to  
875 stratigraphic and hydrocarbon determination, in Payton, C. E., Ed., *Seismic stratigraphy—application to*  
876 *hydrocarbon exploration: AAPG Memoir*, 26, 301–327.

877

878 Taner, M. T., Schuelke, J. S., O'Doherty, R., and Baysal, E., 1994, Seismic attributes revisited: 64th  
879 Ann. Internat. Mtg., Soc. Expl. Geophys., Expanded Abstracts, 1104–1106

880

881 Tedeschi et al., 2017. New age constraints on Aptian evaporites and carbonates from the South  
882 Atlantic: Implications for Oceanic Anoxic Event 1a: *Geology*, doi:10.1130/G38886.1.

883

884 Vail, P.R., Todd, R.G. & Sangree, J.B., 1977. Seismic Stratigraphy and Global Changes of Sea Level,  
885 Part 5: Chronostratigraphy Significance of Seismic Reflections. In: Payton, C. E. (ed.). *Seismic*  
886 *Stratigraphy – Applications to Hydrocarbon Exploration*. Tulsa, *AAPG Memoir* 26, p. 99-116.

887

888 Vinther, R., K. Mosegaard, K. Kierkegaard, I. Abatzis, C. Andersen, O. Vejbaek, F. If, and P. Nielsen,  
889 1995, Seismic texture classification: A computer-aided approach to stratigraphic analysis: 65th Annual  
890 International Meeting, Society of Exploration Geophysicists Expanded Abstracts, v. 95, p. 153–155.

891

892 Zalán, P. V., M. d. C. G. Severino, C. A. Rigoti, L. P. Magnavita, J. A. B. De Oliveira, and A. R. Vianna  
893 2011, An entirely new 3D-view of the crustal and mantle structure of a South Atlantic Passive Margin—  
894 Santos, Campos and Espírito Santo Basins, Brazil, in AAPG Annual Convention and Exhibition,  
895 Houston, Texas.

896

897 Weszka, J., Dyer, C., Rosenfeld, A., 1976. A comparative study of texture measures for terrain  
898 classification. IEEE Trans.Systems Man Cybernet. 6, 269–285.

899

900 Winter, W. R.; Jahnert, R. J.; França, A. B. 2007. Bacia de Campos. Boletim de Geociências da  
901 Petrobras, Rio de Janeiro. v. 15, n. 2, p. 511-529.

902

903 Zhang, Z., and M. Simaan, 1989, Knowledge-based reasoning in SEISIS: A rules-based system for  
904 interpretation of seismic sections based on texture, in F. Aminzadeh and M. Simaan, eds., Expert  
905 systems in exploration: Society of Exploration Geophysicists Geophysical Development Series, v. 3, p.  
906 141–159.

907

#### 908 **Figure captions:**

909 Figure 1: a) Location of the study area offshore Campos Basin, southeastern Brazil. b)  
910 Seismic grid of the 2D lines analyzed for this studies. In bold the location of the three seismic  
911 lines (A, Band C) selected and the two well data |(A and B) utilized for this studies.

912 Figure 2 : Schematic table representing : the main lithostratigraphic units, seismic stratigraphy  
913 units recognized and proposed in this study, the main regional tectonic framework and the  
914 super-sequences (sensu Winter, 2001) for comparison. The color within the seismic  
915 stratigraphy units represents the main mapped horizon and unconformity as represent in the  
916 seismic line interpreted.

917 Figure 3. a) seismic image indicating a Red Green and Blue (RGB) blend of three main  
918 frequencies (20 Hz red, 48 Hz green, 70 Hz Blue Hertz). In white are represented the area  
919 with concentration of the three frequencies. The yellow arrow points respectively the top and  
920 the bottom of the salt unit. The white arrow point the main coquinas unit.b; representationof  
921 part of the Well B calibrating some of the reflectors within the sub-salt Lagoa Feia. The white  
922 points represents the interval velocity from check shot data (2519m/sec; 2402 m/sec). Rge

923 bold number represent the thickness of a single reflection. The color legend represent the  
924 principal lithological information observed from well core data released.

925 Figure 4 Synthetic overview of the various attributes applied (Sweetness; RMS; Cosine of the  
926 phase; RMS amplitude; Relative Acoustic Impedance) and a description of their utility and  
927 interpretation rules within our seismic facies analysis is represented.

928 . Figure 5: A. Seismic line A represent as amplitude expression with 3x vertical exaggeration.  
929 White line represent the main rift faults. Numbers 1, 2 and 3 represent respectively the three  
930 faults family: late syn-rift west dipping fault; 2. Syn-rift east dipping faults. 3. Syn rift listric  
931 fault. Mapped horizons from youngest to oldest: red the post rift unconformity; blue;  
932 maximum rifting surface; yellow the half graben development surface; B. Seismic line B and  
933 the main Well B representing the main lithological units; The white and yellow numbers  
934 (1,2 and 3) as pointed by the white arrows across the all image 5a to c represents areas  
935 characterized by distinctive reflection terminations respect to the main syn-rift fault system.  
936 The yellow number shows the location of the sub-sections. Subsection 1) Reflectors on-  
937 lapping on the west dipping syn rift fault. Subsection 2) Lateral thickening reflectors but on-  
938 lapping on a chaotic zone bordering the syn-rift fault. Subsection 3) reflector on-lapping on  
939 the main fault but concordant respect to the top Cabiunas formation; C. Seismic line A  
940 crossed by the well A and well C.

941 Figure 6. Representation, imaging and description of the main seismic facies (1 to 4)  
942 observed and recognized in the sub- salt Campos Basin.

943 Figure 7 a, b . Seismic attributes images extracted and zoomed from the seismic line A  
944 represented in figure 6. a) seismic image represented as relative acoustic impedance. Note the  
945 clear and distinctive seismic facies 2 and 3 defined by the different brightness and continuity.  
946 b) seismic image (a) expressed as cosine of the phase. Note the facies 2, 3 now characterized  
947 by distinctive thickness and continuity properties.

948 Figure 8 Seismic line C (4x vertically exaggerated) and crossed by the well A. showing the  
949 distribution of the main seismic facies 1,2 and 3. Numbers 1, 2 and 3 represent the units  
950 characterized by the proposed facies 1, 2 and 3. The dotted lines represent the boundaries of  
951 the main seismic facies.

952 Figure 9 Seismic line B with the location of the well B and the mapped seismic facies (1-3)

953 Figure 10 Seismic line A with the location of the well B and the mapped seismic facies (1-3)

954 Figure 11 . Enlarged view of the seismic line 2 (see figure 10) with the location of the well B.

955 In orange are represented the conglomerate and arenitic sandstone; in blue and aquamarine  
956 the coarse grained/rudstone carbonate/coquinas unit; in pale green silty argillite; strong green  
957 the shale and grey the marly units. The basalts in the Cabiúnas Formation are marked with  
958 the purple colour.

959 Figure 12 Representation of the main facies across the Seismic line A. In orange is  
960 represented the seismic facies 1; In green the seismic facies 2; In blu the seismic facies 3.

961 Figure 13 Kinematic restoration test of Line A. a) Mapped normal faults and main units of  
962 the pre-salt interval, corresponding to described systems tracts and seismic facies referred to  
963 in the text. B) Pre-rifting geometries with dashed fault locations. C) Scenario 1, in which  
964 Fault set 2 pre –dates Fault 3 and depositional geometries of the lower part of the lagoa Feia  
965 Fm are largely controlled by Fault Set. d) Scenario 2: kinematically linked fault sets, in which  
966 Fault set 2 branches off a detachment floor fault, which may be linked to Fault 3. e) Border  
967 fault 3 zone formation, with Seismic Facies q related to slump deposits and possible hanging-  
968 wall collapse. f) Activation of Fault Set 1, which post-dates movement on other fault  
969 populations and the deposition of the Lagoa Feia Fm.

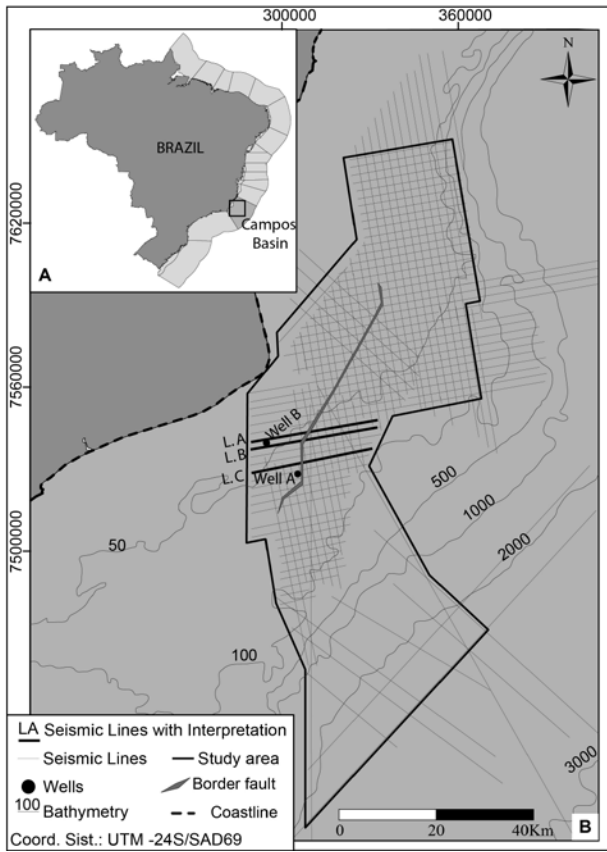
970 Figure 14: Schematic sections of the major sub basin structures mapped in the Campos Basin  
971 . A) the large scale normal fault/rift related structures as mapped from the seismic dataset. In  
972 green the trace representing the main sections shown in B. B) Some examples of the rift  
973 structures and their syn/post rift units mapped and interpreted in this work. In yellow the rift  
974 initiation system track, blue: high tectonic activity system track; purple: low tectonic activity  
975 systems tract. Green: the SAG/salt units.; pale blue: passive margin units; white: sea water.

976

977

978

979



980

981 Fig 1

Litho-stratigraphy	Age Ma	Stratigraphic Framework This Paper	Rifting Process	Super Sequence
Sea		Sea <span style="float: right;">Sea bottom</span>		
Campos Macae r		<b>Passive Margin</b>	Post - Rift	Drift
Retiro Salt	113	<span style="float: right;">Salt base</span>		
L a g o a  F e l i a g r	118/ 124	<b>SAG?</b> Pre salt-base sag unconformity? Surface		Post-rift ??
		<b>Low Tectonic Activity system Tract</b>		
	undef	<span style="float: right;">Tectonic change Surface</span>		
Itabapoana Form (Atafona/ Coqueiros Form equivalent)		<b>High Tectonic Activity System Tract</b>	Syn-Rift	Rift
		<span style="float: right;">Half graben development surface</span>		
Cabiunas V V V V Fm V V V V	130	<b>Rift Initiation System Tract</b> <span style="float: right;">Cabiunas top</span>		
	135/ 540	<span style="float: right;">Pre-rift unconformity</span>		
Basement		<b>PRE-RIFT</b>	Pre-Rift	

982

983

984 Fig 2

985

986

987

988

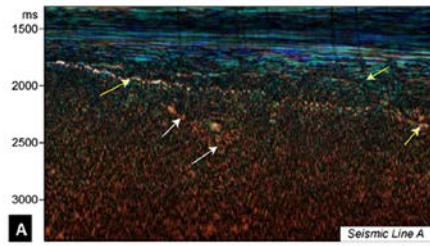
989

990

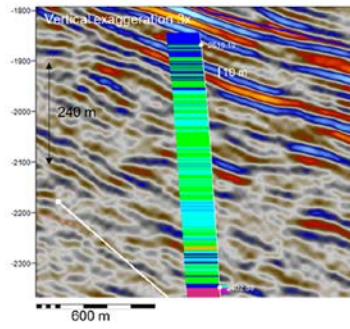
991

992

993



- |  |  |
|--|--|
| <span style="display: inline-block; width: 15px; height: 15px; background-color: #90EE90; border: 1px solid black; margin-right: 5px;"></span> Silty-argillite | <span style="display: inline-block; width: 15px; height: 15px; background-color: #4682B4; border: 1px solid black; margin-right: 5px;"></span> Calcilitite |
| <span style="display: inline-block; width: 15px; height: 15px; background-color: #FF8C00; border: 1px solid black; margin-right: 5px;"></span> Conglomerate    | <span style="display: inline-block; width: 15px; height: 15px; background-color: #ADD8E6; border: 1px solid black; margin-right: 5px;"></span> Calcarenite |
| <span style="display: inline-block; width: 15px; height: 15px; background-color: #008000; border: 1px solid black; margin-right: 5px;"></span> Shale           | <span style="display: inline-block; width: 15px; height: 15px; background-color: #0000FF; border: 1px solid black; margin-right: 5px;"></span> Coquina     |
| <span style="display: inline-block; width: 15px; height: 15px; background-color: #FFFF00; border: 1px solid black; margin-right: 5px;"></span> Arenite         | <span style="display: inline-block; width: 15px; height: 15px; background-color: #800080; border: 1px solid black; margin-right: 5px;"></span> Gypsum/Salt |
| <span style="display: inline-block; width: 15px; height: 15px; background-color: #FF00FF; border: 1px solid black; margin-right: 5px;"></span> Basalt/diabase  | <span style="display: inline-block; width: 15px; height: 15px; background-color: #D8BFD8; border: 1px solid black; margin-right: 5px;"></span> Marl        |



994

995 Fig 4

996

997

998

999

1000

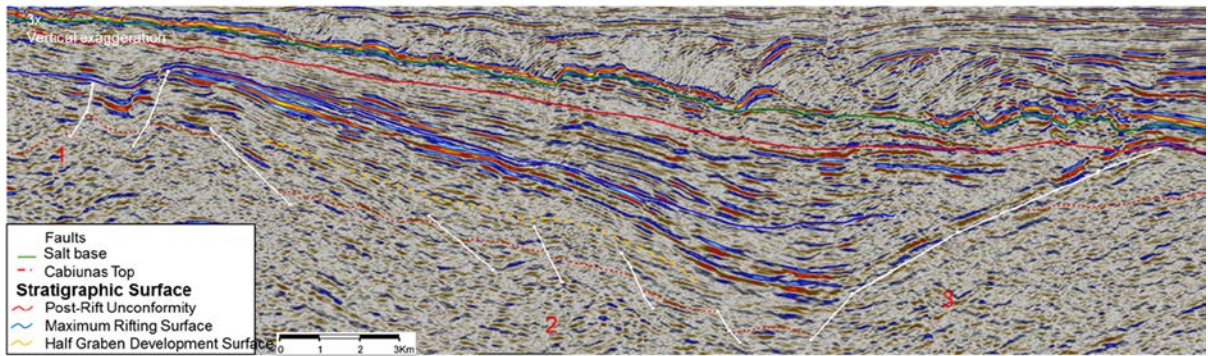
1001

1002

1003

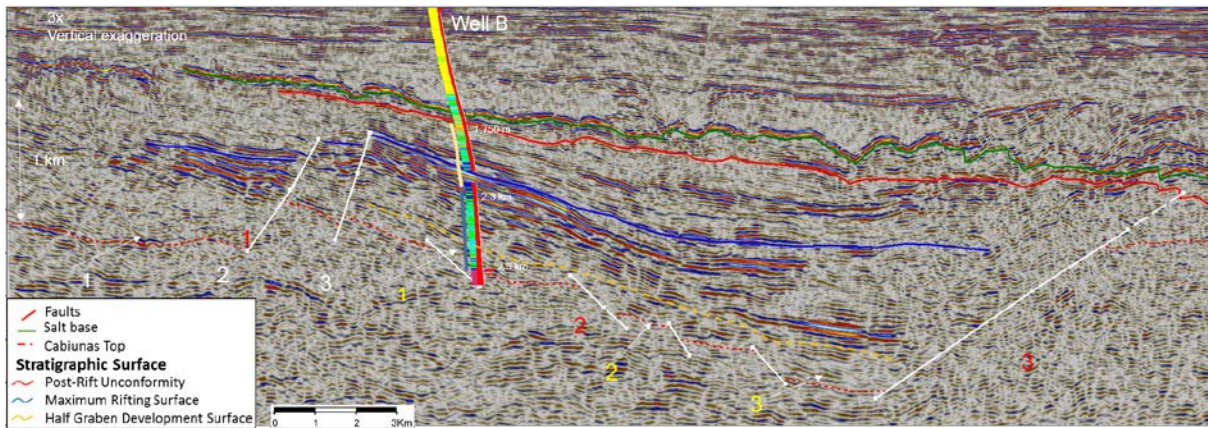
1004



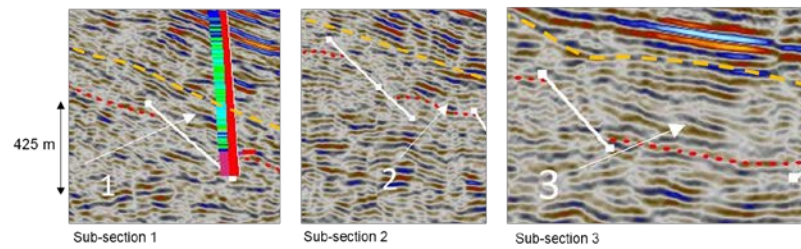


1005

1006 Fig 5a



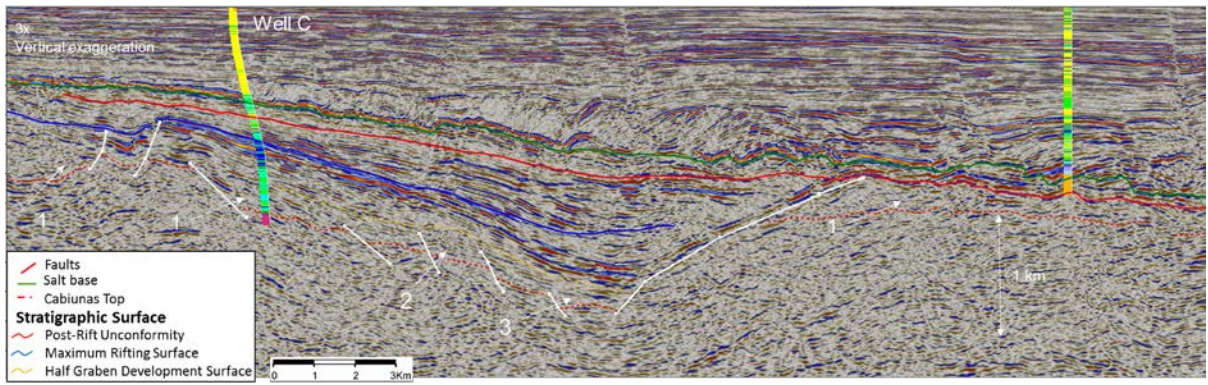
5B Line B



1007

1008 Fig 5b

1009



1010

1011

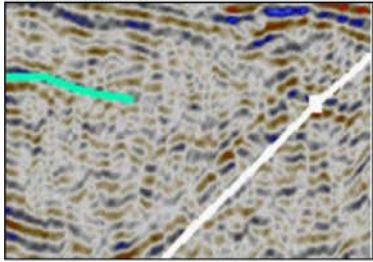
1012 Fig 5c

1013

1014

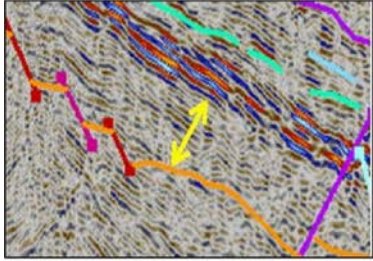
1015

**TEXTURE 1**



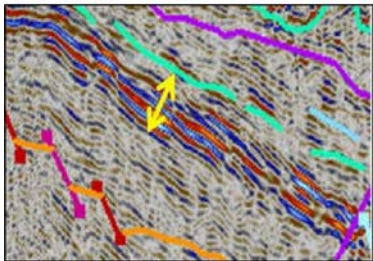
- Chaotic, discontinuous and low-amplitude reflectors amplitude strongly damaged.
- Small vertical faults damaging the units
- Usually juxtaposed to fault plane or lower rift units.

**TEXTURE 2**



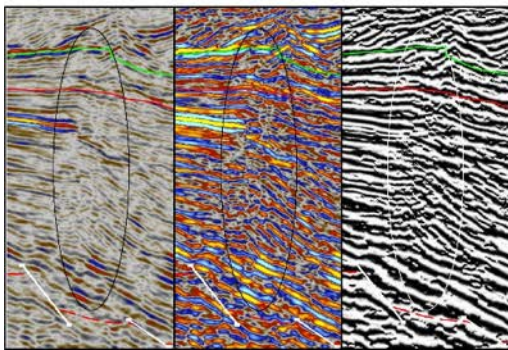
- Semi-continuous reflection, interbedded w/ strong reflections
- Thin layering with lateral low- to medium-amplitude variation
- The unit defined is onlapping or/and slightly lateral thickening on small Rift faults.
- Localized amplitude anomalies.
- Mostly observed within the rift initiation system tract, low- and high-tectonic activity system tract

**TEXTURE 3**



- Very continuous, fat and strong reflectors interbedded w/ thin-layered units, sometimes floating on it.
- The units are rarely laterally thickening.
- Mostly coincident with the rudstone/grainstone units

**TEXTURE 4**



- Pull up velocity effect;
- Wipe out zones with strong discontinuity of the layering and amplitude reduction effects.

1016

1017

1018 Fig 6

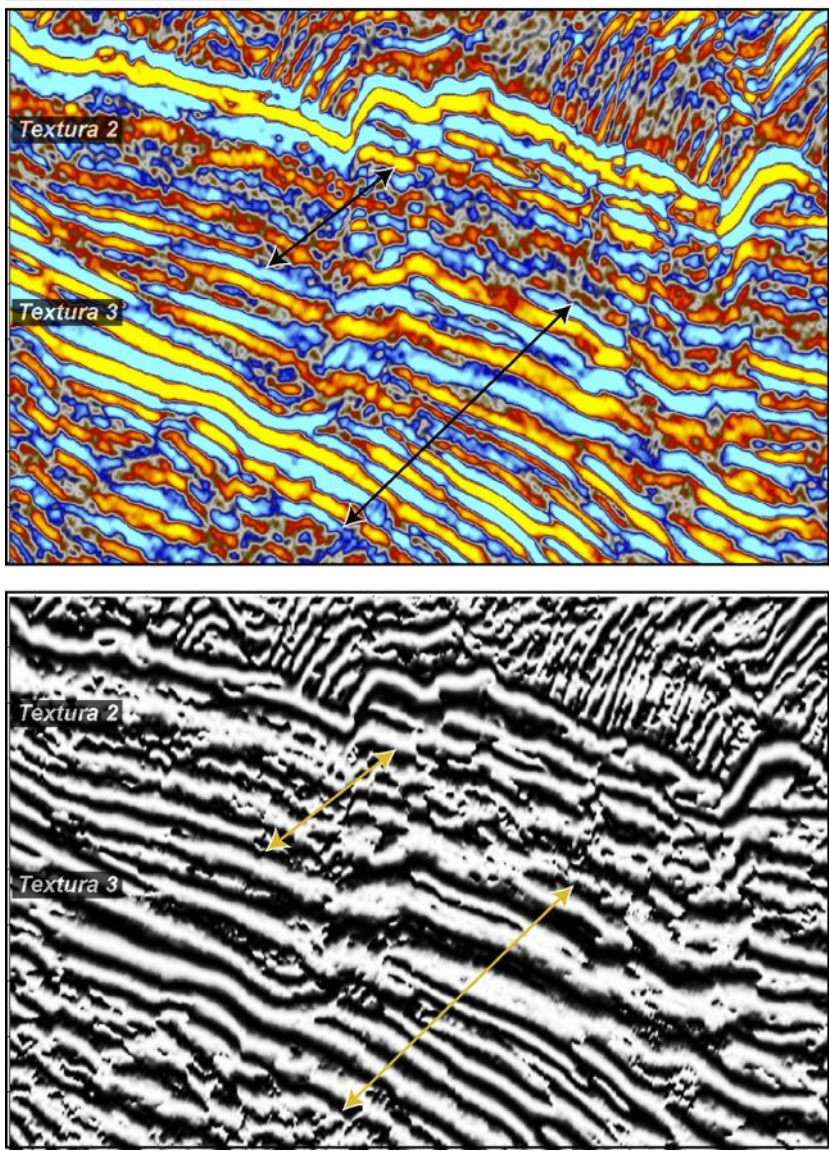
1019

1020

1021

1022

Seismic Line A



1023

1024

1025 Fig 7

1026

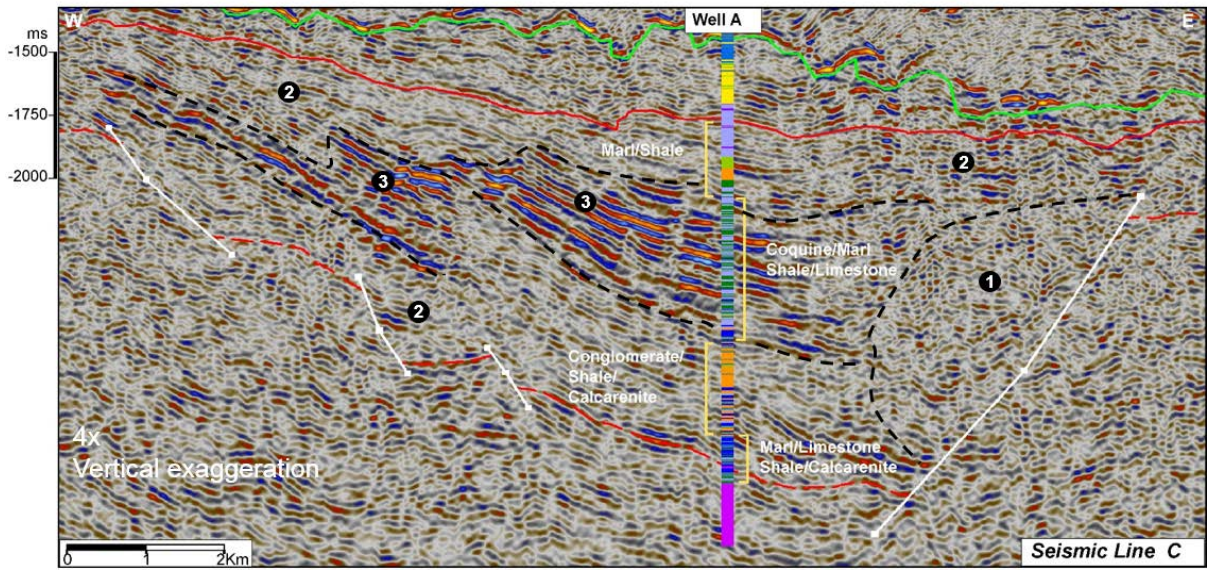
1027

1028

1029

1030

1031

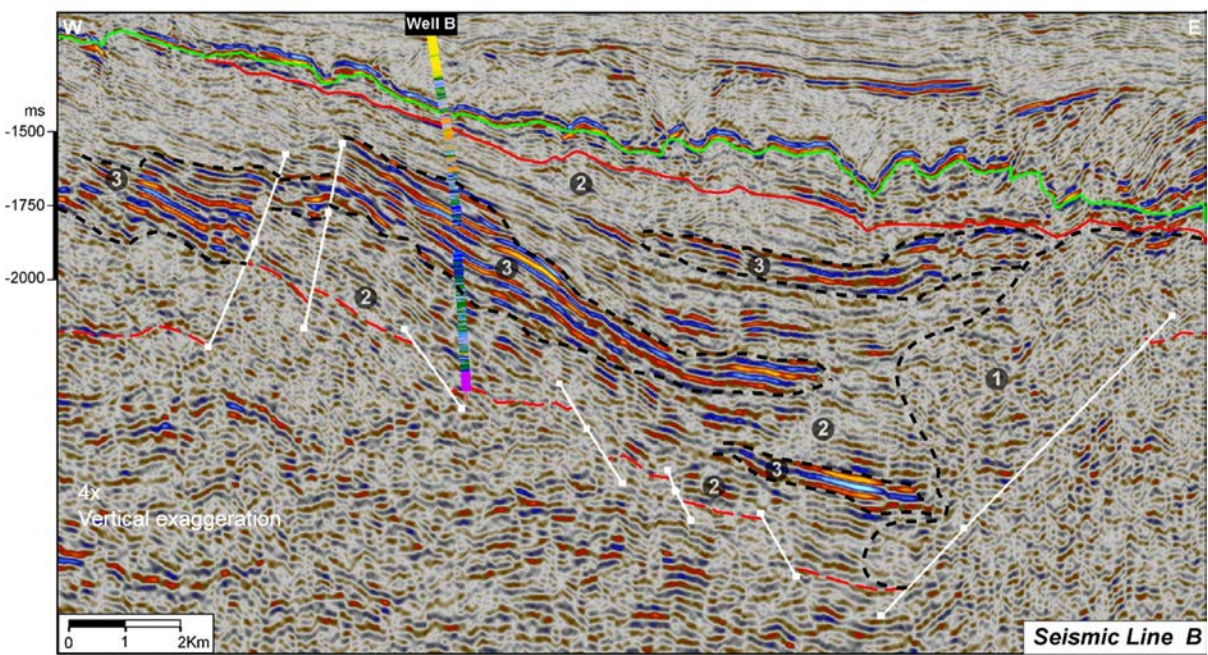


1032

1033

1034 Fig 8

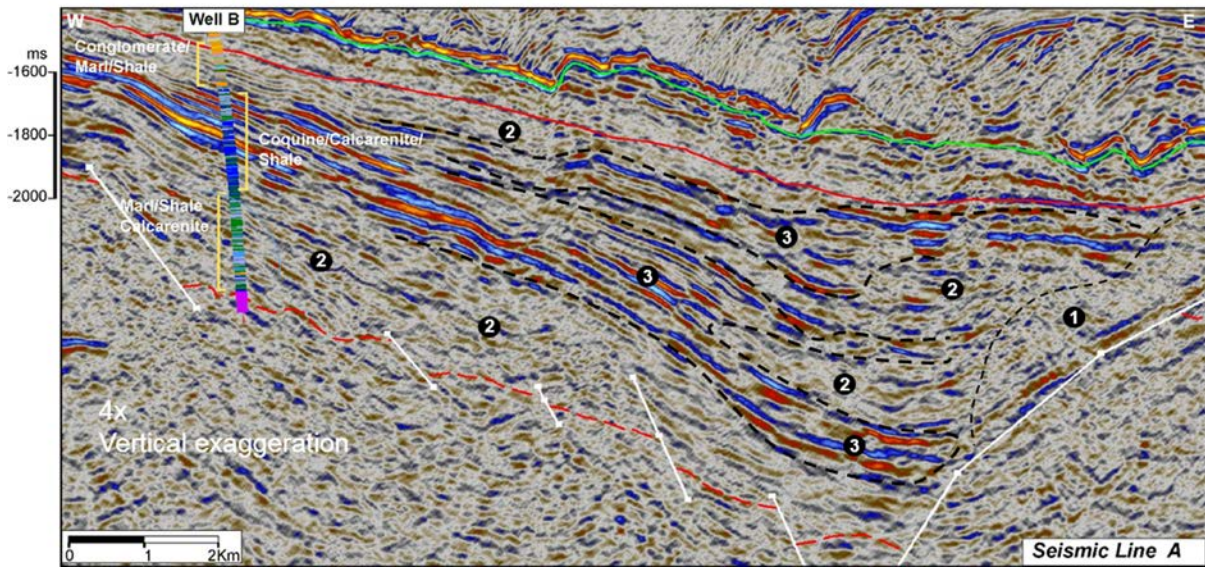
1035



1036

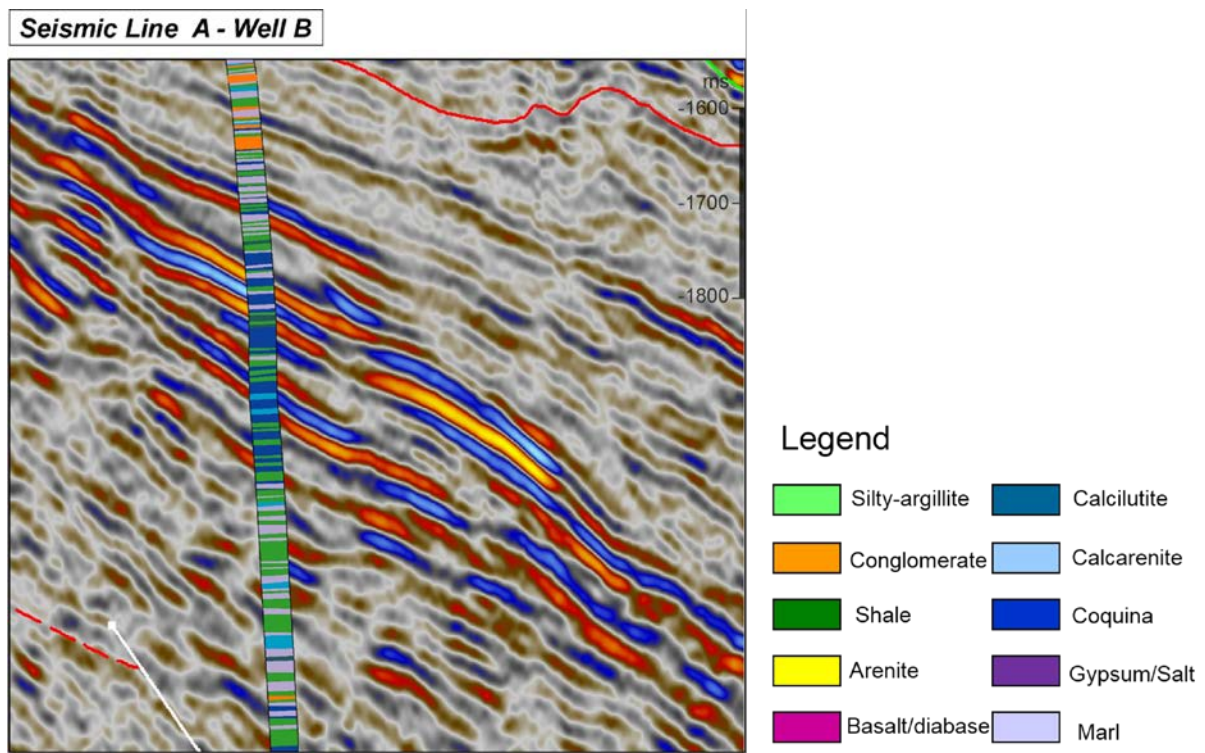
1037 Fig 9

1038



1039

1040 Fig 10

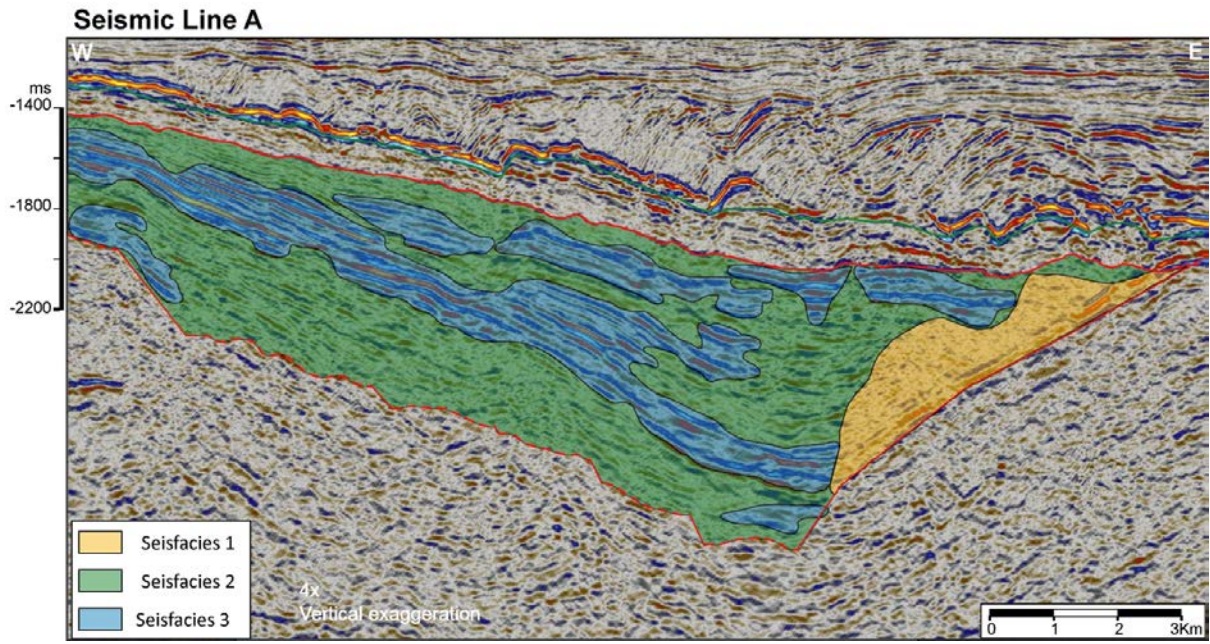


1041

1042 Fig 11

1043

1044



1045

1046

1047 Fig 12

1048

1049

1050

1051

1052

1053

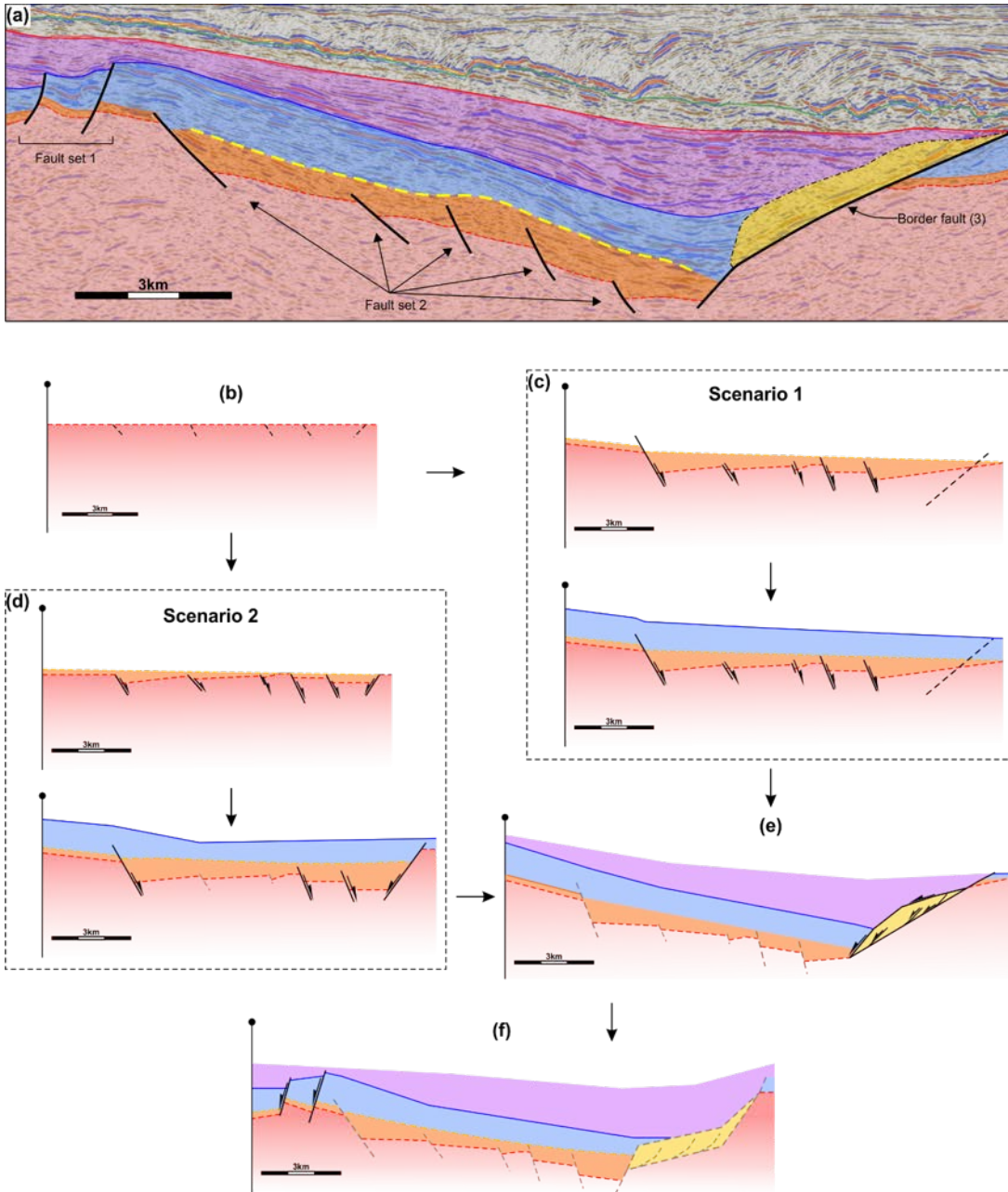
1054

1055

1056

1057

1058



1059

1060 Fig 13

1061

1062

1063

1064



